

# Resonant Slepton Production in Hadron–Hadron Collisions

H. Dreiner<sup>\*1</sup>, P. Richardson<sup>†2</sup>, and M. H. Seymour<sup>\*3</sup>

*\* Rutherford Appleton Laboratory, Chilton, Didcot OX11 0QX, U.K.*

*† Department of Physics, Theoretical Physics, University of Oxford,  
1 Keble Road, Oxford OX1 3NP, United Kingdom*

## Abstract

We consider the resonant production of sleptons via  $\mathcal{R}_p$  in hadron–hadron collisions followed by supersymmetric gauge decays of the sleptons. We look at decay modes which lead to the production of a like-sign dilepton pair. The dominant production mechanism giving this signature is the resonant production of a charged slepton followed by a decay to a charged lepton and a neutralino which then decays via  $\mathcal{R}_p$ . The discovery potential of this process at Run II of the Tevatron and the LHC is investigated using the HERWIG Monte Carlo event generator. We include the backgrounds from the MSSM. We conclude with a discussion of the possibility of extracting the lightest neutralino and slepton masses.

---

<sup>1</sup>E-mail address: H.K.Dreiner@rl.ac.uk

<sup>2</sup>E-mail address: p.richardson1@physics.ox.ac.uk

<sup>3</sup>E-mail address: M.Seymour@rl.ac.uk

# 1 Introduction

In the R-parity violating ( $\mathcal{R}_p$ ) extension of the Minimal Supersymmetric Standard Model (MSSM) [1] supersymmetric particles can be produced on resonance. While the cross sections for these resonant production processes are suppressed by the  $\mathcal{R}_p$  Yukawa couplings, the kinematic reach is greater than that of supersymmetric particle pair production.

The  $\mathcal{R}_p$  extension to the MSSM contains the following additional terms in the superpotential

$$\mathbf{W}_{\mathcal{R}_p} = \frac{1}{2}\lambda_{ijk}\varepsilon^{ab}L_a^iL_b^j\bar{E}^k + \lambda'_{ijk}\varepsilon^{ab}L_a^iQ_b^j\bar{D}^k + \frac{1}{2}\lambda''_{ijk}\varepsilon^{\alpha\beta\gamma}\bar{U}_\alpha^i\bar{D}_\beta^j\bar{D}_\gamma^k + \kappa_iL_iH_2, \quad (1)$$

where  $i, j = 1, 2, 3$  are the generation indices,  $a, b = 1, 2$  are the  $SU(2)_L$  indices and  $\alpha, \beta, \gamma = 1, 2, 3$  are the  $SU(3)_C$  indices.  $L^i$  ( $Q^i$ ) are the lepton (quark)  $SU(2)$  doublet superfields,  $\bar{E}^i$  ( $\bar{D}^i, \bar{U}^i$ ) are the electron (down and up quark)  $SU(2)$  singlet superfields, and  $H_n$ ,  $n = 1, 2$ , are the Higgs superfields. For a recent summary of the bounds on the couplings in Eqn. 1 see [2].

The terms in Eqn. 1 lead to different resonant production mechanisms in various collider experiments. The first term leads to resonant sneutrino production in  $e^+e^-$  collisions [3–9], while the third term gives resonant squark production in hadron–hadron collisions [10–17]. The second term gives both resonant squark production in ep collisions [18] and resonant slepton production in hadron–hadron collisions, which we will consider here.

	Charged Sleptons	Sneutrinos
Supersymmetric	$\tilde{\ell}_{i\alpha} \rightarrow \ell_i^- \tilde{\chi}^0$	$\tilde{\nu}_i \rightarrow \nu_i \tilde{\chi}^0$
Gauge Decays	$\tilde{\ell}_{i\alpha} \rightarrow \nu_i \tilde{\chi}^-$	$\tilde{\nu}_i \rightarrow \ell_i^- \tilde{\chi}^+$
$\mathcal{R}_p$ Decays	$\tilde{\ell}_{i\alpha} \rightarrow \bar{u}_j d_k$ $\tilde{\ell}_{i\alpha} \rightarrow \bar{\nu}_j \ell_k^-$	$\tilde{\nu}_i \rightarrow \bar{d}_j d_k$ $\tilde{\nu}_i \rightarrow \ell_j^+ \ell_k^-$
Weak Decays	$\tilde{\ell}_{i\alpha} \rightarrow \tilde{\nu}_i W^-$ $\tilde{\ell}_{i2} \rightarrow \tilde{\ell}_{i1} Z_0$	$\tilde{\nu}_i \rightarrow \tilde{\ell}_{i\alpha} W^+$
Higgs Decays	$\tilde{\ell}_{i\alpha} \rightarrow \tilde{\nu}_i H^-$ $\tilde{\ell}_{i2} \rightarrow \tilde{\ell}_{i1} h_0, H_0, A_0$	$\tilde{\nu}_i \rightarrow \tilde{\ell}_{i\alpha} H^+$

Table 1: Decay modes of charged sleptons and sneutrinos. The index  $\alpha = 1, 2$  gives the mass eigenstate of the slepton.

A systematic study of  $\mathcal{R}_p$  signatures at hadron colliders was first performed in [11]. Resonant slepton production in hadron–hadron collisions has previously been considered in [10–13, 19–23]. The signature of this process depends on the decay mode of the resonant slepton. The various possible decay channels are given in Table 1. Most of the previous studies have considered only the  $\mathcal{R}_p$  decays of the resonant slepton to either leptons via the first term in Eqn. 1 [10, 13, 19, 20], or to quarks via the second term in Eqn. 1 [10, 12, 13, 20].

There has been no study of the supersymmetric gauge decays of the resonant charged sleptons. The cross sections for these processes were first presented in [10] where there was a discussion of the possible experimental signatures, however the signal we are considering was not discussed and there was no calculation of the Standard Model background. In several workshop contributions we have presented first studies of the supersymmetric gauge decays of charged sleptons [13, 21, 23]. Here we present a complete analysis of both the Tevatron and LHC case. The supersymmetric gauge decays of sneutrinos have been studied in [22, 23]. These studies were performed using a hadron-level Monte Carlo simulation for both the signal and background processes, in addition the analyses of [22, 23] used a detector simulation and looked at the trilepton signature for resonant sneutrino production.

We will consider a specific signature, *i.e.* like-sign dilepton production, for these processes rather than any one given resonant production mechanism. We would expect like-sign dilepton production to have a low background from Standard Model (SM) processes. This is an extension of our analysis of [13, 21, 23] to include additional signal processes and Standard Model backgrounds. We also consider the background from sparticle pair production and the possibility of measuring the sparticle masses which was not considered in [13, 21, 23]. We use a parton-shower Monte Carlo simulation, including hadronization but no detector simulation, for both the signal and background processes.

In Section 2 we will consider the signal processes in more detail, followed by a discussion of the various different processes which contribute to the background in Section 3. We will also discuss the various cuts which can be used to reduce the background. In Section 4 we will then consider the discovery potential at both Run II of the Tevatron and at the LHC. We also consider the possibility of reconstructing the neutralino and slepton masses using their decay products.

## 2 Signal

There are a number of different possible production mechanisms for a like-sign dilepton pair via resonant slepton production. The dominant production mechanism is the production of a charged slepton followed by a supersymmetric gauge decay of the charged slepton to a neutralino and a charged lepton. This neutralino can then decay via the crossed process to give a second charged lepton, which due to the Majorana nature of the neutralino can have the same charge as the lepton produced in the slepton decay. The production of a charged lepton and a neutralino via the LQD term in the  $\mathcal{R}_p$  superpotential, Eqn. 1, occurs at tree-level via the Feynman diagrams given in Fig. 1. The decay of the neutralino occurs at tree-level via the diagrams given in Fig. 2.

Like-sign dileptons can also be produced in resonant charged slepton production with a supersymmetric gauge decay of the slepton to a chargino and neutrino,  $\ell^+ \rightarrow \tilde{\chi}_1^+ \nu_\ell$ . The chargino can then decay  $\tilde{\chi}_1^+ \rightarrow \ell^+ \nu_\ell \tilde{\chi}_1^0$ . Again, given the majorana nature of the neutralino, it can decay to give a like-sign dilepton pair.

The production of like-sign dileptons is also possible in resonant sneutrino production followed by a supersymmetric gauge decay to a chargino and a charged lepton,  $\tilde{\nu} \rightarrow \ell^- \tilde{\chi}_1^+$ .

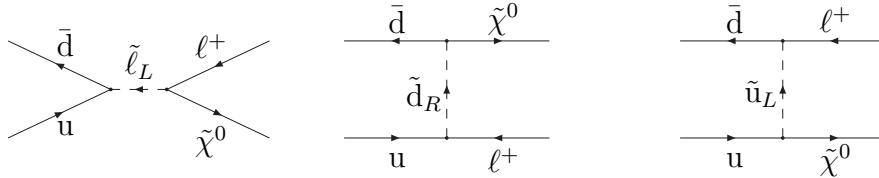


Figure 1: Production of  $\tilde{\chi}^0 \ell^+$ .

This can be followed by  $\tilde{\chi}_1^+ \rightarrow q\bar{q}'\tilde{\chi}_1^0$ , the neutralino can then decay as in Fig. 2 to give a like-sign dilepton pair.

All the resonant  $\mathcal{R}_p$  production mechanisms and the decays of the SUSY particles have been included in the HERWIG event generator [24]. The implementation of both R-parity conserving and R-parity violating SUSY is described in [25], the matrix elements used for the various  $\mathcal{R}_p$  processes are given in [12].

We will only consider one of the  $\mathcal{R}_p$  Yukawa couplings to be non-zero at a time. We shall focus on  $\lambda'_{211}$ , which leads to resonant smuon production. The production cross-section depends quadratically on the  $\mathcal{R}_p$  Yukawa coupling. The low-energy bound is given by

$$\lambda'_{211} < 0.059 \times \left( \frac{M_{\tilde{d}_R}}{100\text{GeV}} \right), \quad (2)$$

from the ratio  $R_\pi = \Gamma(\pi \rightarrow e\nu_e)/\Gamma(\pi \rightarrow \mu\nu_\mu)$  [2, 4]. The bound on the coupling  $\lambda'_{111}$  from neutrino-less double beta decay [2, 26] is very strict and basically excludes an observable signal. For higher generation couplings  $\lambda'_{2ij}$  the cross section is suppressed by low parton luminosities. We do not consider the production of  $\tau$  leptons.

As we are considering a dominant  $\lambda'_{211}$  coupling the leptons produced in the neutralino decays and the hard processes will be muons. We will therefore require throughout that both leptons are muons because this reduces the background, where electrons and muons are produced with equal probability, with respect to the signal. This typically reduces the Standard Model background by a factor of four while leaving the dominant signal process almost unaffected. It will lead to some reduction of the signal from channels where some of the leptons are produced in cascade decays from the decay of a W or Z boson.

The signal has a number of features, in addition to the presence of a like-sign dilepton pair, which will enable us to extract it above the background:

- Provided that the difference between the slepton and the neutralino/chargino masses is large enough both the leptons will have a high transverse momentum,  $p_T$ , and be well isolated.
- As the neutralino decays inside the detector, for this signature, there will be little missing transverse energy,  $\cancel{E}_T$ , in the event. Any  $\cancel{E}_T$  will come from semi-leptonic hadron decays or from cascade decays following the production of a chargino or one of the heavier neutralinos.

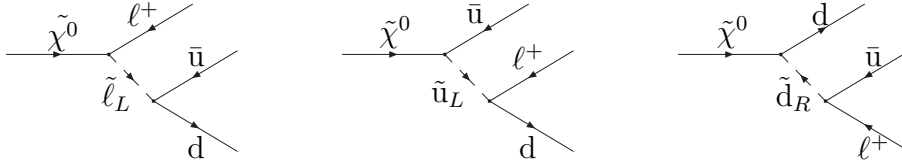


Figure 2: Feynman diagrams for the decay  $\tilde{\chi}^0 \rightarrow \ell^+ d \bar{u}$ . The neutralino is a Majorana fermion and decays to the charge conjugate final state as well. There is a further decay mode  $\tilde{\chi}^0 \rightarrow \nu d \bar{d}$ .

- The presence of a third lepton can only come from semi-leptonic hadron decays, or in SUSY cascade decays if a chargino or one of the heavier neutralinos is produced.
- The presence of two hard jets from the decay of the neutralino.

The cross section for the signal processes and the acceptance<sup>1</sup> will depend upon the various SUSY parameters. Due to the large number of parameters we will use the standard minimal SUGRA scenario where the soft SUSY breaking masses for the gauginos ( $M_{1/2}$ ) and scalars ( $M_0$ ), and the tri-linear SUSY breaking terms ( $A_0$ ) are universal at the GUT scale. In addition we require radiative electroweak symmetry breaking. This leaves five parameters  $M_{1/2}$ ,  $M_0$ ,  $A_0$ ,  $\tan\beta$  and  $\text{sgn}\mu$ .

We have performed a scan in  $M_0$  and  $M_{1/2}$  with  $A_0 = 0$  GeV for two different values of  $\tan\beta$  and both values of  $\text{sgn}\mu$ . The masses of the left-handed smuon and the lightest neutralino are shown in Fig. 3. There are regions in these plots which we have not considered either due to the lack of radiative electroweak symmetry breaking, or because the lightest neutralino is not the lightest supersymmetric particle (LSP). In the MSSM, the LSP must be a neutral colour singlet [27], from cosmological bounds on electric- or colour-charged stable relics. However if R-parity is violated the LSP can decay and these bounds no longer apply. We should therefore consider cases where one of the other SUSY particles is the LSP. We have only considered the case where the neutralino is the LSP for two reasons:

1. Given the unification of the SUSY breaking parameters at the GUT scale it is hard to find points in parameter space where the lightest neutralino is not the LSP without the lightest neutralino becoming heavier than the sleptons, which tend to be the lightest sfermions in these models. If the neutralino is heavier than the sleptons the resonance will not be accessible for the supersymmetric gauge decay modes we are considering and the slepton will decay via  $\tilde{R}_p$  modes.
2. The ISAJET code for the running of the couplings and the calculation of the MSSM decay modes only works when the neutralino is the LSP.

The plots in Fig. 3 also include the current experimental limits on the SUSY parameters from LEP. This experimentally excluded region comes from two sources: the region at large  $M_0$  is excluded by the limit on the cross section for chargino pair production from [28] and

<sup>1</sup>We define the acceptance to be the fraction of signal events which pass the cuts.

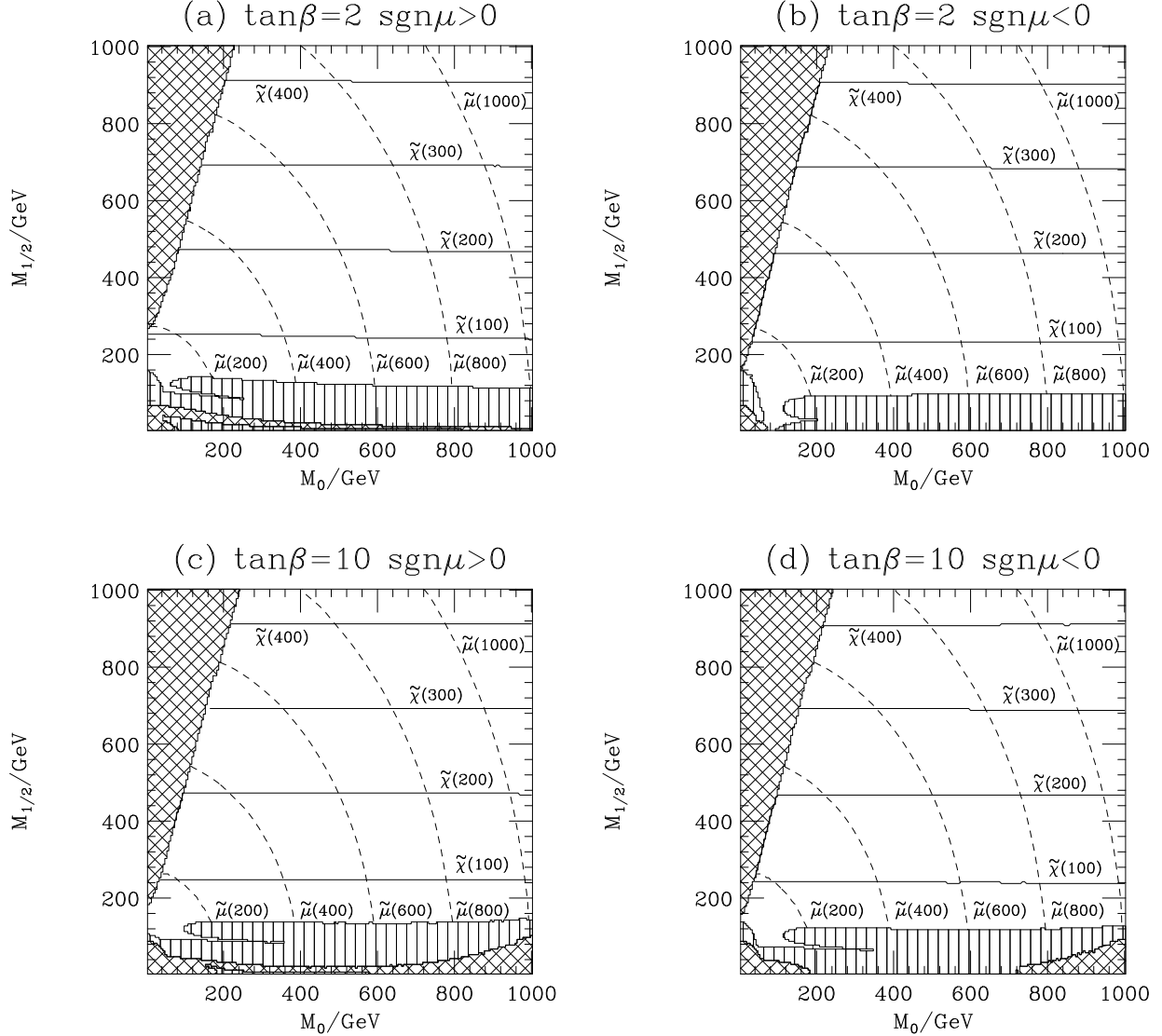


Figure 3: Contours showing the lightest neutralino mass, solid lines, and the  $\tilde{\mu}_L$  mass, dashed lines, in the  $M_0$ ,  $M_{1/2}$  plane with  $A_0 = 0$  GeV for different values of  $\tan\beta$  and  $\text{sgn}\mu$ . The hatched regions at small  $M_0$  are excluded by the requirement that the  $\tilde{\chi}_1^0$  be the LSP. The region at large  $M_0$  and  $\tan\beta$  is excluded because there is no radiative electroweak symmetry breaking. The vertically striped region is excluded by the LEP experiments. This was obtained using the limits on the chargino [28] and smuon [29] production cross sections, and the chargino mass [30]. This analysis was performed using ISAJET 7.48 [31].

the limit on the chargino mass from [30]; the region at small  $M_0$  is excluded by the limit on the production of smuons from [29]. There is also a limit on the neutralino production cross section from [28], however for most of the SUGRA parameter space this is weaker than the limit on chargino pair production. The gap in the excluded region between  $M_0$  of about 50 GeV and 100 GeV is due to the presence of a destructive interference between the  $t$ -channel sneutrino exchange and the  $s$ -channel photon and  $Z$  exchanges in the chargino production cross section in  $e^+e^-$  collisions.

The limit on the coupling  $\lambda'_{211}$  is shown in Fig. 4. As can be seen from Figs. 3 and 4 the limit on the coupling is fairly weak for large regions of parameter space, even when the smuon is relatively light. This is due to the squark masses, upon which the limit depends, being larger than the slepton masses, in the SUGRA models (*c.f.* Eq.2).

The signature we are considering requires the neutralino to decay inside the detector. In practice, if the neutralino decays more than a few centimeters from the primary interaction point a different analysis including the displaced vertices would be necessary. The neutralino decay length is shown in Fig. 5 and is small for all the currently allowed values of the SUGRA parameters. There will however be a lower limit on the  $\mathcal{R}_p$  couplings which can be probed using this process as the decay length  $\sim 1/\lambda'^2_{211}$  [32].

## 3 Backgrounds

### 3.1 Standard Model Backgrounds

The dominant Standard Model backgrounds to like-sign dilepton production come from:

- Gauge boson pair production, *i.e.* production of  $WZ$  or  $ZZ$  followed by leptonic decays with some of the leptons not being detected.
- $t\bar{t}$  production. Either the  $t$  or  $\bar{t}$  decays semi-leptonically, giving one lepton. The second top decays hadronically. A second lepton with the same charge can be produced in a semi-leptonic decay of the bottom hadron formed in the decay of the second top, *i.e.*

$$\begin{aligned} t &\rightarrow W^+b \rightarrow \mu^+\bar{\nu}_\mu b, \\ \bar{t} &\rightarrow W^-\bar{b} \rightarrow q\bar{q}\bar{b}, \quad \bar{b} \rightarrow \mu^+\bar{\nu}_\mu\bar{c}. \end{aligned} \tag{3}$$

- $b\bar{b}$  production. If either of these quarks hadronizes to form a  $B_{d,s}^0$  meson this can mix to give a  $\bar{B}_{d,s}^0$ . This means that if both the bottom hadrons decay semi-leptonically the leptons will have the same charge as they are both coming from either  $b$  or  $\bar{b}$  decays.
- Single top production. A single top quark can be produced together with a  $\bar{b}$  quark by either an  $s$ - or  $t$ -channel  $W$  exchange. This can give one charged lepton from the top decay, and a second lepton with the same charge from the decay of the meson formed after the  $b$  quark hadronizes.

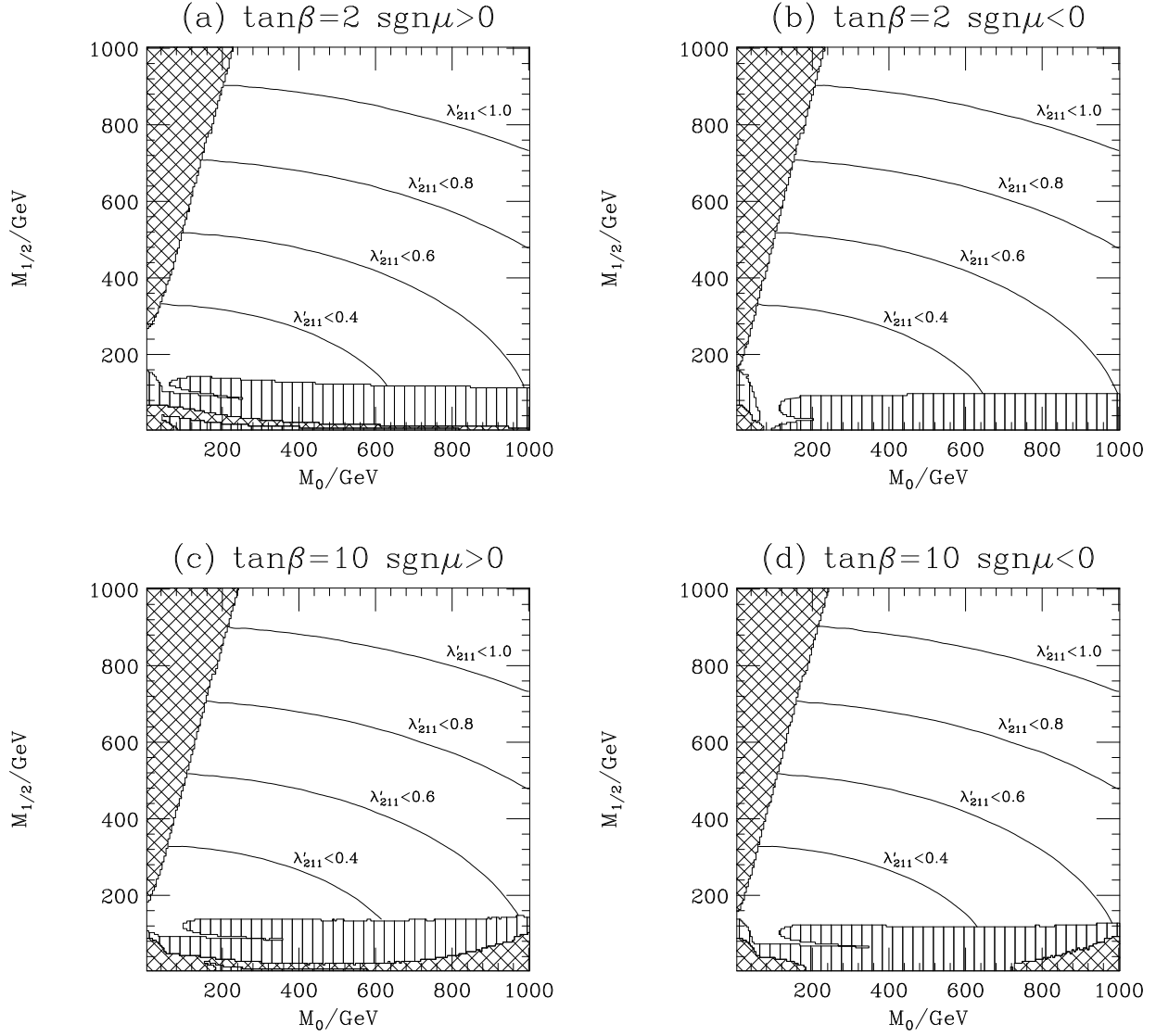


Figure 4: Contours showing the limit on the  $\mathcal{R}_p$  Yukawa coupling  $\lambda'_{211}$  in the  $M_0$ ,  $M_{1/2}$  plane for  $A_0 = 0$  GeV and different values of  $\tan\beta$  and  $\text{sgn}\mu$ . The striped and hatched regions are the same as in Fig. 3.



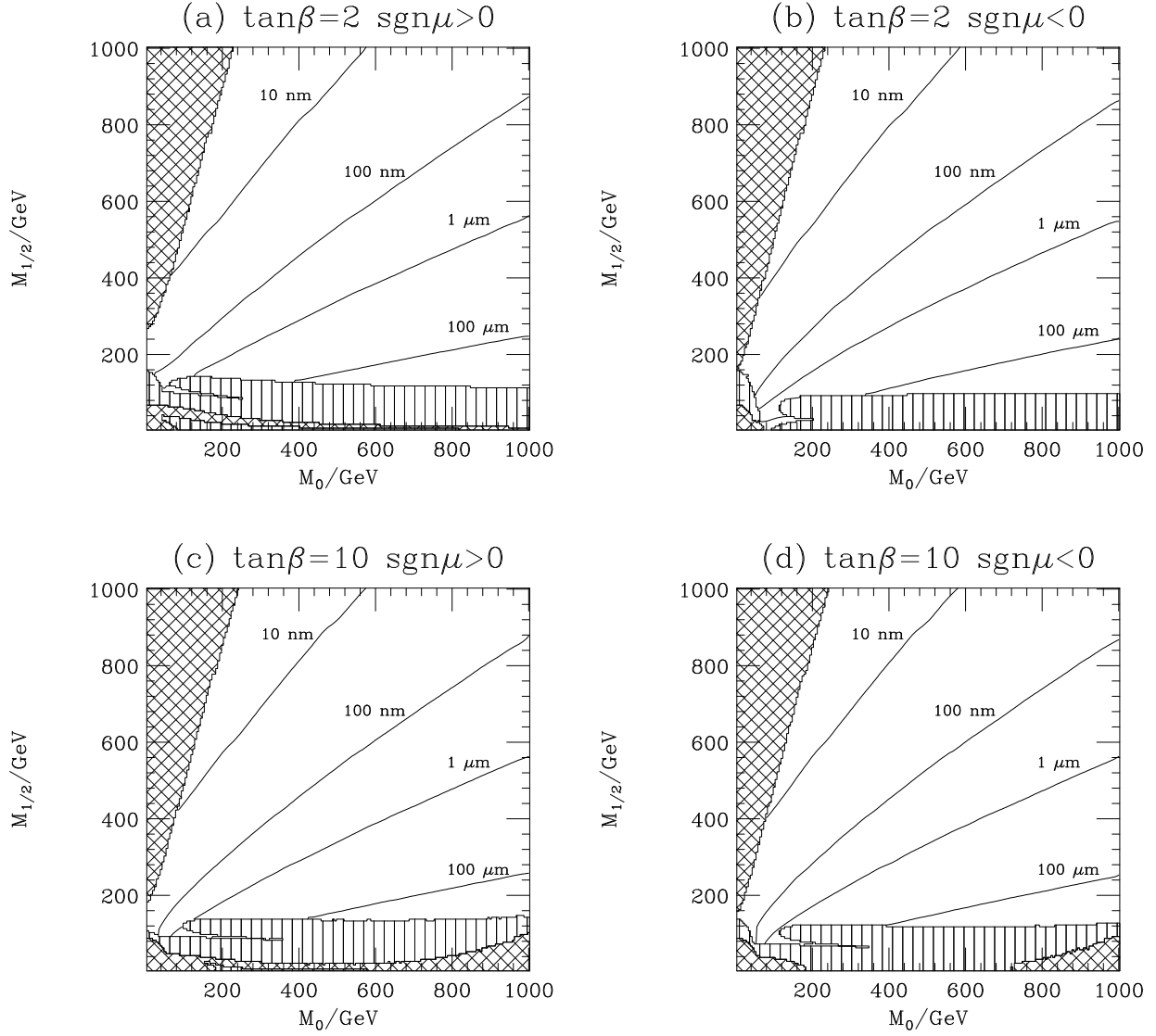


Figure 5: Contours showing the decay length of a neutralino produced in the decay of an on-mass-shell slepton in the  $M_0$ ,  $M_{1/2}$  plane for  $A_0 = 0$  GeV,  $\lambda'_{211} = 10^{-2}$  and different values of  $\tan\beta$  and  $\text{sgn}\mu$ . The striped and hatched regions are the same as in Fig. 3.

- Non-physics backgrounds. There are two major sources: (i) from misidentifying the charge of a lepton, *e.g.* in Drell-Yan production, and (ii) from incorrectly identifying an isolated hadron as a lepton. This means that there is a major source of background from W production with an additional jet faking a lepton.

These processes have been extensively studied [33–45] as they are also the major backgrounds to the production of like-sign dileptons in the MSSM. The first studies of like-sign dilepton production at the LHC [37] only considered the background from heavy quark production, *i.e.*  $t\bar{t}$  and  $b\bar{b}$  production. More recent studies for both the LHC [38–41] and Run II of the Tevatron [42–45] have also considered the background from gauge boson pair production. In addition the Tevatron studies [42–45] have included the non-physics backgrounds. We have considered all the physics backgrounds, from both heavy quark production and gauge boson pair production, but have neglected the non-physics backgrounds which would require a full simulation of the detector. As we discuss below, since our signal is different, the optimal cuts are also different in our case.

In these studies a number of different cuts have been used to suppress the backgrounds. These cuts can be split into two groups, firstly those cuts which are designed to reduce the background from heavy quark production:

- A cut on the  $p_T$  of the leptons requiring

$$p_T^{\text{lepton}} > p_T^{\text{CUT}}. \quad (4)$$

The values of  $p_T^{\text{CUT}}$  for Tevatron studies have been between 5 and 20 GeV. Higher values, between 20 and 50 GeV, have usually been used in LHC simulations.

- A cut requiring that the leptons are isolated, *i.e.* imposing a cut on the transverse energy,  $E_T^{IC}$ , in a cone about the direction of the lepton such that

$$E_T^{IC} < E_0. \quad (5)$$

$E_0$  has usually been taken to be less than 5 GeV for Tevatron simulations and between 5 and 10 GeV for LHC studies. The radius of the cone is usually taken to be

$$\Delta R = \sqrt{\Delta\phi^2 + \Delta\eta^2} < 0.4, \quad (6)$$

where  $\Delta\phi$  is the azimuthal angle and  $\Delta\eta$  the pseudo-rapidity of the particles with respect to the lepton.

It was shown in [37] that these cuts can reduce the background from heavy quark production by several orders of magnitude. Any high  $p_T$  lepton from a bottom hadron decay must come from a high  $p_T$  hadron. This is due to the small mass of the bottom hadron relative to the lepton  $p_T$  which means the lepton will be travelling in the same direction as the other decay products [46]. Hence the isolation and  $p_T$  cuts remove the majority of these events.

The analyses of [40–45] then imposed further cuts to reduce the backgrounds from gauge boson pair production, which is the major contribution to the SM background after the imposition of the isolation and  $p_T$  cuts:

- A cut on the invariant mass,  $m_{\ell+\ell^-}$ , of any pair of opposite sign same flavour (OSSF) leptons to remove those leptons coming from Z decays, *i.e.*

$$|M_Z - m_{\ell+\ell^-}| < m_{\ell+\ell^-}^{\text{CUT}}, \quad (7)$$

was used in the analyses of [42, 44, 45].

- Instead of a cut on the mass of OSSF lepton pairs some analyses considered a veto on the presence of an OSSF lepton pair in the event.
- In [43, 45] a cut on the transverse mass was imposed to reject leptons which come from the decays of W bosons. The transverse mass,  $M_T$ , of a lepton neutrino pair is given by

$$M_T^2 = 2|p_{T_\ell}||p_{T_\nu}|(1 - \cos \Delta\phi_{\ell\nu}), \quad (8)$$

where  $p_{T_\ell}$  is the transverse momentum of the charged lepton,  $p_{T_\nu}$  is the transverse momentum of the neutrino (assumed to be the total missing transverse momentum in the event) and  $\Delta\phi_{\ell\nu}$  is the azimuthal angle between the lepton and the neutrino, *i.e.* the missing momentum in the event. This cut is applied to both of the like-sign leptons in the event to reject events in which either of them came from the decay of a W boson. A cut removing events with  $60 \text{ GeV} < M_T < 85 \text{ GeV}$  was used in [45] to reduce the background from WW and WZ production.

- For the MSSM signatures considered in [42–45] there is missing transverse energy,  $\cancel{E}_T$ , due to the LSP escaping from the detector. This allowed them to impose a cut on the  $\cancel{E}_T$ ,  $\cancel{E}_T > E_T^{\text{CUT}}$ , to reduce the background.

There are however differences between the MSSM signatures which were considered in [42–45] and the  $\mathcal{R}_p$  processes we are considering here. In particular as the LSP decays, there will be little missing transverse energy in the  $\mathcal{R}_p$  events. This means that instead of a cut requiring the  $\cancel{E}_T$  to be above some value we will consider a cut requiring the  $\cancel{E}_T$  to be less than some value, *i.e.*

$$\cancel{E}_T < E_T^{\text{CUT}}. \quad (9)$$

This cut will remove events from some of the possible resonant production mechanisms, *i.e.* those channels where a neutrino is produced in either the slepton decay or the cascade decay of a chargino, or one of the heavier neutralinos, to the lightest neutralino. However it will not affect the decay of a charged slepton to a neutralino which is the dominant production mechanism over most of the SUSY parameter space.

Similarly, the signal we are considering in general will not contain more than two leptons. Further leptons can only come from cascade decays following the production of either a chargino or one of the heavier neutralinos, or from semi-leptonic hadron decays. This means that instead of the cut on the invariant mass of OSSF lepton pairs we will only consider the effect of a veto on the presence of OSSF pairs. This veto was considered in [42, 43] but for the MSSM signal considered there it removed more signal than background.

## 3.2 SUSY backgrounds

So far we have neglected what may be the major source of background to this process, *i.e.* supersymmetric particle pair production. If we only consider small  $\mathcal{R}_p$  couplings the dominant effect in sparticle pair production is that the LSP produced at the end of the cascade decays of the other SUSY particles will decay. For large  $\mathcal{R}_p$  couplings the cascade decay chains can also be affected by the heavier SUSY particles decaying via  $\mathcal{R}_p$  modes, which we will not consider here.<sup>2</sup> The LSP will decay giving a quark-antiquark pair and either a charged lepton or a neutrino. There will usually be two LSPs in each event, one from the decay chain of each of the sparticles produced in the hard collision. This means that they can both decay to give leptons with the same charge. Leptons can also be produced in the cascade decays. These processes will therefore be a major background to like-sign dilepton production via resonant slepton production.

The cuts which were intended to reduce the Standard Model background will also significantly reduce the background from sparticle pair production. However we will need to impose additional cuts to suppress this background. In the signal events there will be at least two high  $p_T$  jets from the neutralino decay, there may be more jets from either initial-state QCD radiation or radiation from quarks produced in the neutralino decay. In the dominant production mechanism, *i.e.*  $\tilde{\mu} \rightarrow \mu^- \tilde{\chi}_1^0$ , this will be the only source of jets, however additional jets can be produced in the cascade SUSY decays if a chargino or one of the heavier neutralinos is produced. In the SUSY background there will be at least four high  $p_T$  jets from the neutralino decays, plus other jets formed in the decays of the coloured sparticles which are predominantly formed in hadron-hadron collisions. This suggests two possible strategies for reducing the sparticle pair production background:

1. A cut such that there are at most 2 or 3 jets (allowing for some QCD radiation) above a given  $p_T$ . This will reduce the SUSY background which typically has more than four high  $p_T$  jets.
2. A cut such that there are exactly two jets, or only two or three jets above a given  $p_T$ . This will reduce the gauge boson pair background where typically the only jets come from initial-state radiation, as well as the background from sparticle pair production.

In practice we would use a much higher momentum cut in the first case, as we only need to ensure that the cut is sufficiently high that most of the sparticle pair production events give more than 2 or 3 jets above the cut. However with the second cut we need to ensure that the jets in the signal have sufficiently high  $p_T$  to pass the cut as well. In practice we found that the first cut significantly reduced the sparticle pair production background while having little effect on the signal, while the second cut dramatically reduced the signal as well. In the next section we will consider the effects of cut 1. on both the signal and background at Run II of the Tevatron and the LHC.

---

<sup>2</sup>These additional decays are included in HERWIG6.1.

## 4 Simulations

HERWIG 6.1 [24] was used to simulate the signal and the backgrounds from sparticle pair,  $t\bar{t}$ ,  $b\bar{b}$  and single top production. HERWIG does not include gauge boson pair production in hadron-hadron collisions and we therefore used PYTHIA 6.1 [47] to simulate this background. The simulation of the signal includes all the non- $\mathcal{R}_p$  decay modes given in Table 1. We used a cone algorithm with  $R = 0.4$  radians for all the jet reconstructions. The algorithm is similar to that used by CDF, apart from using the midpoints between two particles as a seed for the algorithm in addition to the particles themselves. The inclusion of the midpoints as seeds improves the infra-red safety of the cone algorithm.

Due to the large cross sections for some of the Standard Model backgrounds before any cuts we imposed parton-level cuts and forced certain decay modes in order to simulate a sufficient number of events with the resources available. We designed these cuts in such a way that hopefully they are weaker than any final cut we apply, so that we do not lose any of the events that would pass the final cuts. We imposed the following cuts for the various backgrounds:

- $b\bar{b}$  production. We forced the B hadrons produced by the hadronization to decay semi-leptonically. This neglects the production of leptons in charm decays which has a higher cross section but which we would expect to have a lower  $p_T$  and be less well isolated than those leptons produced in bottom decays. If there was only one  $B_{d,s}^0$  meson in the event this was forced to mix. When there was more than one  $B_{d,s}^0$  meson then one of them was forced to mix and the others were forced not to mix. Similarly we imposed a parton-level cut on the transverse momentum of the initial b and  $\bar{b}$ ,  $p_T^{b,\bar{b}} \geq p_T^{\text{parton}}$ . This parton-level cut should not affect the background provided that we impose a cut on the transverse momentum of the leptons produced in the decay,  $p_T^{\text{lepton}} \geq p_T^{\text{parton}}$ .
- $t\bar{t}$  production. While not as large as the  $b\bar{b}$  production cross section the cross section for  $t\bar{t}$  is large, particularly at the LHC. We improved the efficiency by forcing one of the top quarks in each event to decay semi-leptonically, again this neglects events in which there are leptons from charm decay. However we did not impose a cut on the  $p_T$  of the top quarks as due to the large top quark mass even relatively low  $p_T$  top quarks can give high  $p_T$  leptons.
- Single top production. While the cross section for this process is relatively small compared to the heavy quark pair production cross sections we still forced the top to decay semi-leptonically as above to reduce the number of events we need to simulate.
- Gauge Boson Pair Production. The cross sections for these processes are relatively small and it was not necessary to impose any parton-level cuts, or force particular decay modes.

Where possible the results of the Monte Carlo simulations have been normalized by using next-to-leading-order cross sections for the various background processes. We used

the next-to-leading-order calculation of [48] for gauge boson pair production. The  $t\bar{t}$  simulations were normalized using the next-to-leading-order with next-to-leading-log resummation calculation from [49].

The calculation of a next-to-leading-order cross section for  $b\bar{b}$  production is more problematic due to the parton-level cuts we imposed on the simulated events. There are a range of possible options for applying the  $p_T$  cut we imposed on the bottom quark at next-to-leading order. At leading order the transverse momenta of the quarks are identical and therefore the cut requires them both to have transverse momentum  $p_T > p_T^{\text{CUT}}$ . However at next-to-leading order, due to gluon radiation, the transverse momenta of the quarks are no longer equal. Therefore a cut on for example the  $p_T$  of the hardest quark,  $p_{T_1} > p_T^{\text{CUT}}$ , together with a cut on the lower  $p_T$  quark,  $p_{T_2} > p_T^{\text{CUT}} - \delta$ , with any positive value of  $\delta < p_T^{\text{CUT}}$  is the same as the leading-order cut we applied. Given that we need a high transverse momentum bottom hadron to give a high  $p_T$  lepton and only events with two such high  $p_T$  leptons will contribute to the background a cut requiring both bottom quarks to have  $p_T > p_T^{\text{CUT}}$ , *i.e.*  $\delta = 0$ , is most appropriate. However at this point the perturbation theory is unreliable [50] and for the cuts we applied the next-to-leading-order cross section is smaller than the leading-order result. We therefore applied the cut  $p_{T_1} > p_T^{\text{CUT}}$  with no cut on the softer bottom as this avoids the point at which the perturbative expansion is unreliable, *i.e.*  $\delta = p_T^{\text{CUT}}$ . We used the program of [51] to calculate the next-to-leading-order cross section with these cuts.

All of the simulations and SUSY cross section calculations used the latest MRS parton distribution set [52], as did the calculation of the single top production cross section. The parton distribution sets used in the various next-to-leading-order cross sections are described in the relevant papers.

We can now study the signal and background in more detail for both the Tevatron and the LHC. This is followed by a discussion of methods to reconstruct the masses of both the lightest neutralino and the resonant slepton.

## 4.1 Tevatron

The cross section for the production of a neutralino and a charged lepton, which is the dominant production mechanism, is shown in Fig. 6 in the  $M_0, M_{1/2}$  plane with  $A_0 = 0$  GeV and  $\lambda'_{211} = 10^{-2}$  for two different values of  $\tan\beta$  and both values of  $\text{sgn}\mu$ . The total cross section for resonant slepton production followed by supersymmetric gauge decays is shown in Fig 7. As can be seen the total cross section closely follows the slepton mass contours shown in Fig. 3 whereas the neutralino lepton cross section falls-off more quickly at small  $M_{1/2}$  where the charginos and heavier neutralinos can be produced. This cross section must be multiplied by the acceptance, *i.e.* the fraction of signal events which pass the cuts, to give the number of observable events in the experiment.

We will first discuss the cuts applied to reduce the various Standard Model backgrounds and then present the discovery potential at the Tevatron if we only consider these backgrounds. This is followed by a discussion of the additional cuts needed to reduce the background from sparticle pair production.

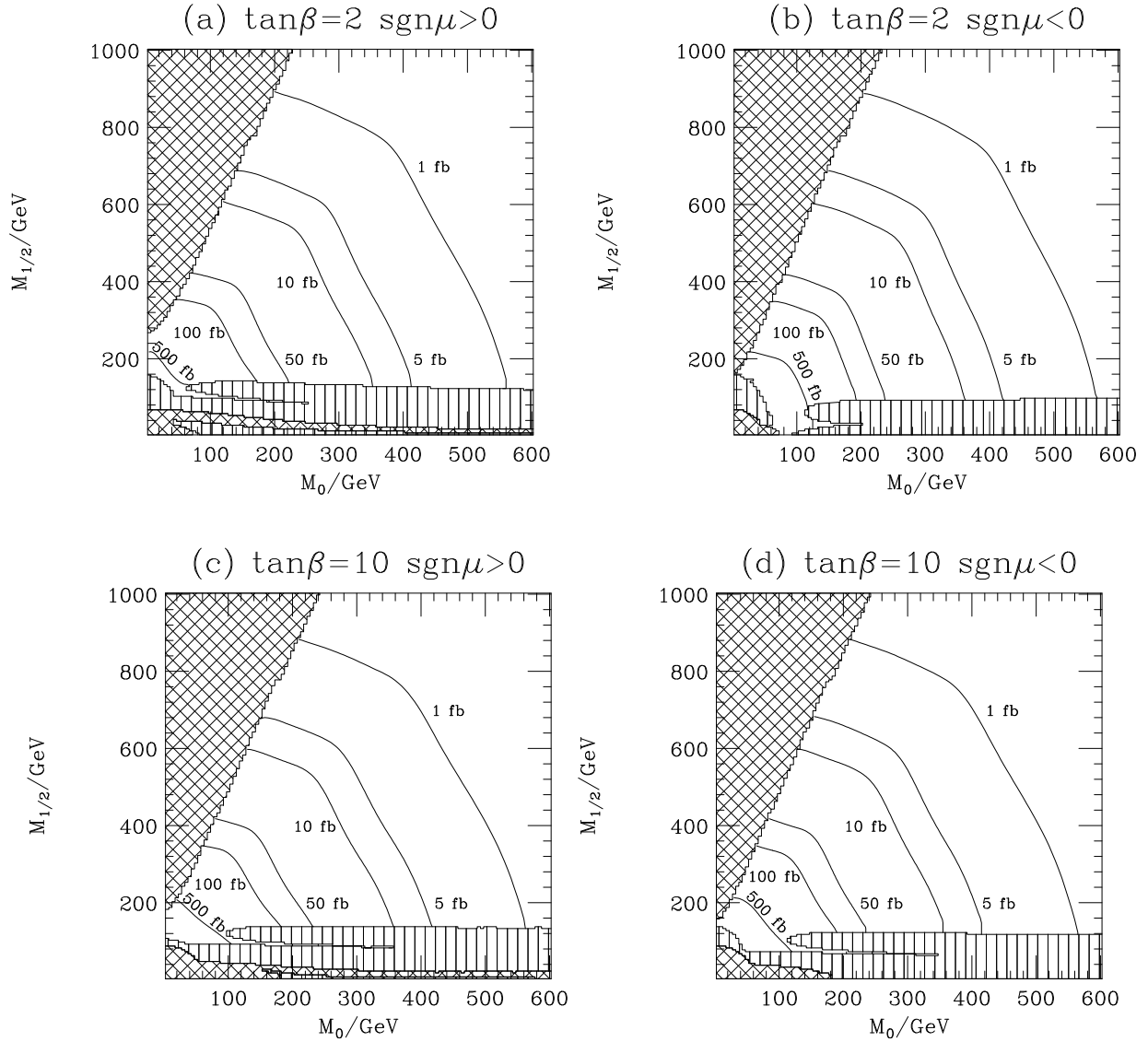


Figure 6: Contours showing the cross section for the production of a neutralino and a charged lepton at Run II of the Tevatron in the  $M_0$ ,  $M_{1/2}$  plane for  $A_0 = 0$  GeV and  $\lambda'_{211} = 10^{-2}$  with different values of  $\tan\beta$  and  $\text{sgn}\mu$ . The striped and hatched regions are described in the caption of Fig. 3.

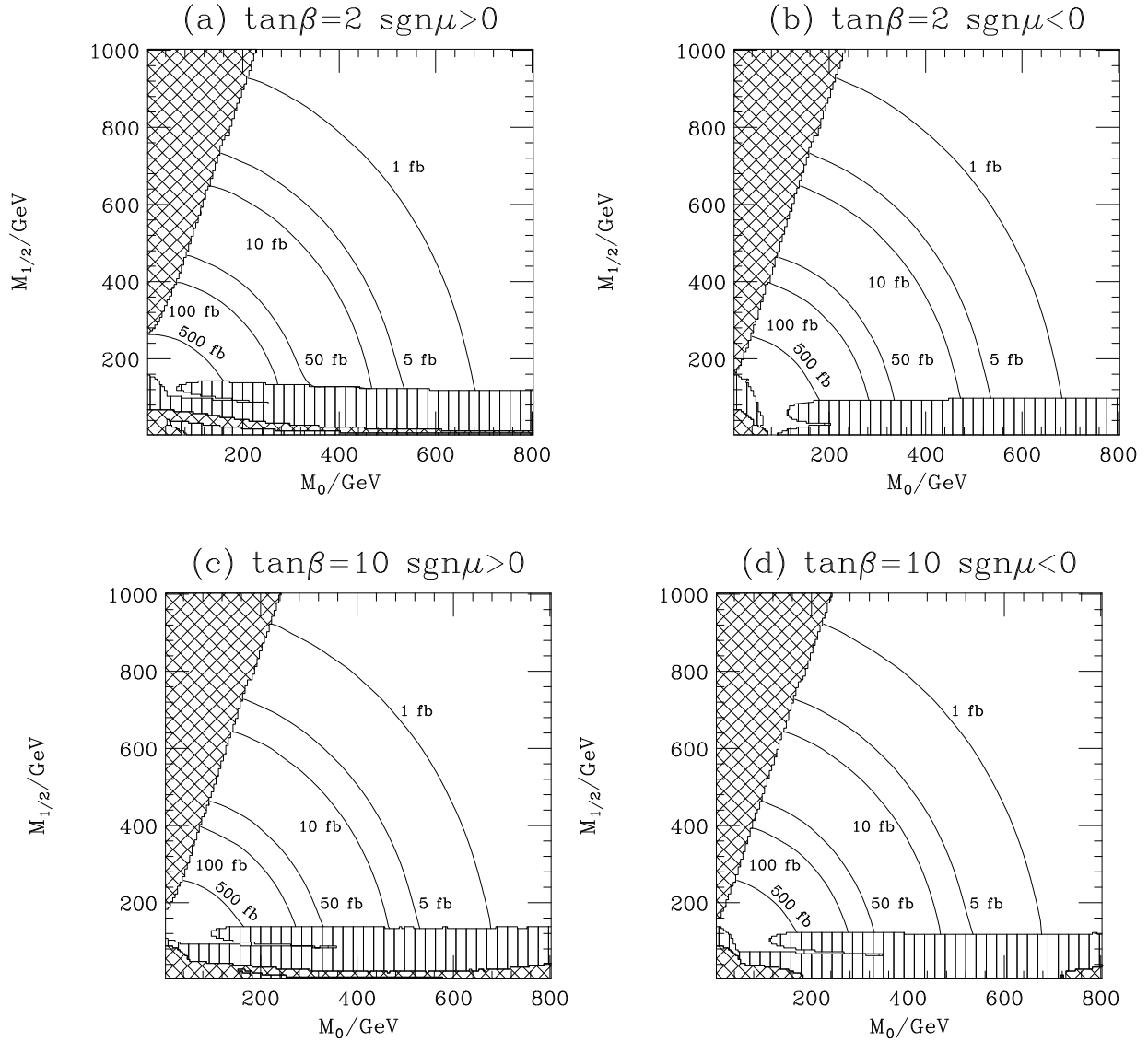


Figure 7: Contours showing the cross section for the production of a slepton followed by a supersymmetric gauge decay at Run II of the Tevatron in the  $M_0, M_{1/2}$  plane for  $A_0 = 0$  GeV and  $\lambda'_{211} = 10^{-2}$  with different values of  $\tan\beta$  and  $\text{sgn}\mu$ . The striped and hatched regions are described in the caption of Fig. 3.



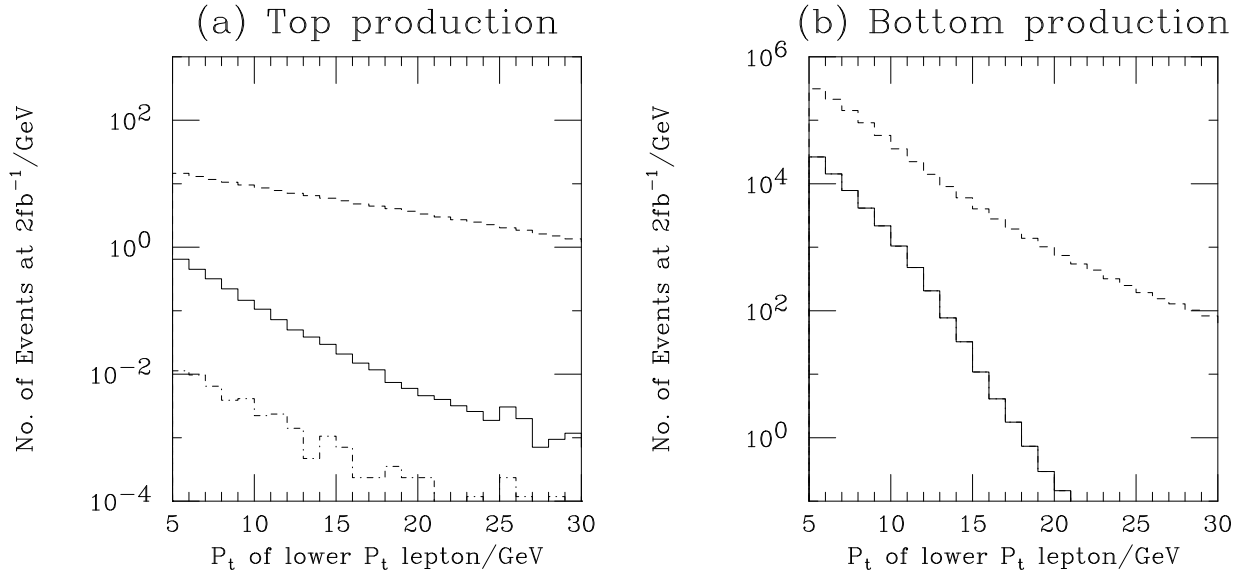


Figure 8: Effect of the isolation cuts on the  $t\bar{t}$  and  $b\bar{b}$  backgrounds at Run II of the Tevatron. The dashed line gives the background before any cuts, the solid line shows the effect of the isolation cut described in the text. The dot-dash line gives the effect of all the cuts, including the cut on the number of jets, for the  $b\bar{b}$  background this is indistinguishable from the solid line. The distributions have been normalized to  $2\text{fb}^{-1}$  integrated luminosity. As a parton-level cut of 20 GeV was used in simulating the  $b\bar{b}$  background the results below 20 GeV for the lepton  $p_T$  do not correspond to the full number of background events.

#### 4.1.1 Standard Model Backgrounds

We have applied the following cuts to reduce the Standard Model backgrounds:

1. A cut requiring all the leptons to be in the central region of the detector,  $|\eta| < 2.0$ .
2. A cut on the transverse momentum of each of the like-sign leptons  $p_T^{\text{lepton}} \geq 20\text{ GeV}$ , this is the lowest cut we could apply given our parton level cut of  $p_T^{\text{parton}} = 20\text{ GeV}$ , for the  $b\bar{b}$  background.
3. An isolation cut on the like-sign leptons so that the transverse energy in a cone of radius,  $R = \sqrt{\Delta\phi^2 + \Delta\eta^2} = 0.4$ , about the direction of the lepton is less than 5 GeV.
4. We reject events with  $60\text{ GeV} < M_T < 85\text{ GeV}$  (*c.f.* Eqn. 8.) This cut is applied to both of the like-sign leptons.
5. A veto on the presence of a lepton in the event with the same flavour but opposite charge as either of the leptons in the like-sign pair if the lepton has  $p_T > 10\text{ GeV}$  and passes the same isolation cut as the like-sign leptons.

Background Process	Number of Events			
	After $p_T$ cut	After isolation and $p_T$ cuts	After isolation, $p_T$ , $M_T$ , $\cancel{E}_T$ cuts and OSSF lepton veto.	After all cuts
WW	$0.23 \pm 0.02$	$0.0 \pm 0.003$	$0.0 \pm 0.003$	$0.0 \pm 0.003$
WZ	$9.96 \pm 0.09$	$7.93 \pm 0.08$	$0.21 \pm 0.01$	$0.21 \pm 0.01$
ZZ	$2.05 \pm 0.03$	$1.61 \pm 0.02$	$0.069 \pm 0.005$	$0.069 \pm 0.005$
$t\bar{t}$	$34.1 \pm 1.6$	$0.028 \pm 0.002$	$0.0032 \pm 0.0006$	$0.0016 \pm 0.0004$
bb	$(3.4 \pm 1.3) \times 10^3$	$0.15 \pm 0.16$	$0.15 \pm 0.16$	$0.15 \pm 0.16$
Single Top	$1.77 \pm 0.01$	$0.0014 \pm 0.0003$	$0.0001 \pm 0.0001$	$0.0001 \pm 0.0001$
Total	$(3.4 \pm 1.3) \times 10^3$	$9.72 \pm 0.18$	$0.43 \pm 0.16$	$0.43 \pm 0.16$

Table 2: Backgrounds to like-sign dilepton production at Run II of the Tevatron. The numbers of events are based on an integrated luminosity of  $2 \text{ fb}^{-1}$ . We have calculated an error on the cross section by varying the scale between half and twice the hard scale, apart from the gauge boson pair production cross section where we do not have this information and the effect of varying the scale is expected to be small anyway. The error on the number of events is then the error on the cross section and the statistical error from the Monte Carlo simulation added in quadrature. If no events passed the cut the statistical error was taken to be the same as if one event had passed the cuts.

6. A cut on the missing transverse energy,  $\cancel{E}_T < 20 \text{ GeV}$ . In our analysis we have assumed that the missing transverse energy is solely due to the momenta of the neutrinos produced.

The first two cuts are designed to reduce the background from heavy quark production, which is the major source of background before any cuts. As can be seen in Fig. 8 the cut on the transverse momentum,  $p_T > 20 \text{ GeV}$ , reduces the background by several orders of magnitude and the addition of the isolation cut reduces this background to less than one event at Run II of the Tevatron.

The remaining cuts reduce the background from gauge boson pair production which dominates the Standard Model background after the imposition of the isolation and  $p_T$  cuts. Fig. 9a shows that the cut on the transverse mass, *i.e.* removing the region  $60 \text{ GeV} < M_T < 85 \text{ GeV}$ , for each of the like-sign leptons will reduce the background from WZ production, which is the largest of the gauge boson pair production backgrounds. Similarly the cut on the missing transverse energy,  $\cancel{E}_T < 20 \text{ GeV}$ , will significantly reduce the background from WZ production as can be seen in Fig. 9b. The effect of these cuts is shown in Fig. 10. Our simulations do not include  $W\gamma$  production which was recently found to be a major source of background to like-sign dilepton production in the MSSM [43]. However, we would expect this to be less important here due to the different cuts we have applied. In particular, in the analysis of [43] a cut on the invariant mass of OSSF lepton

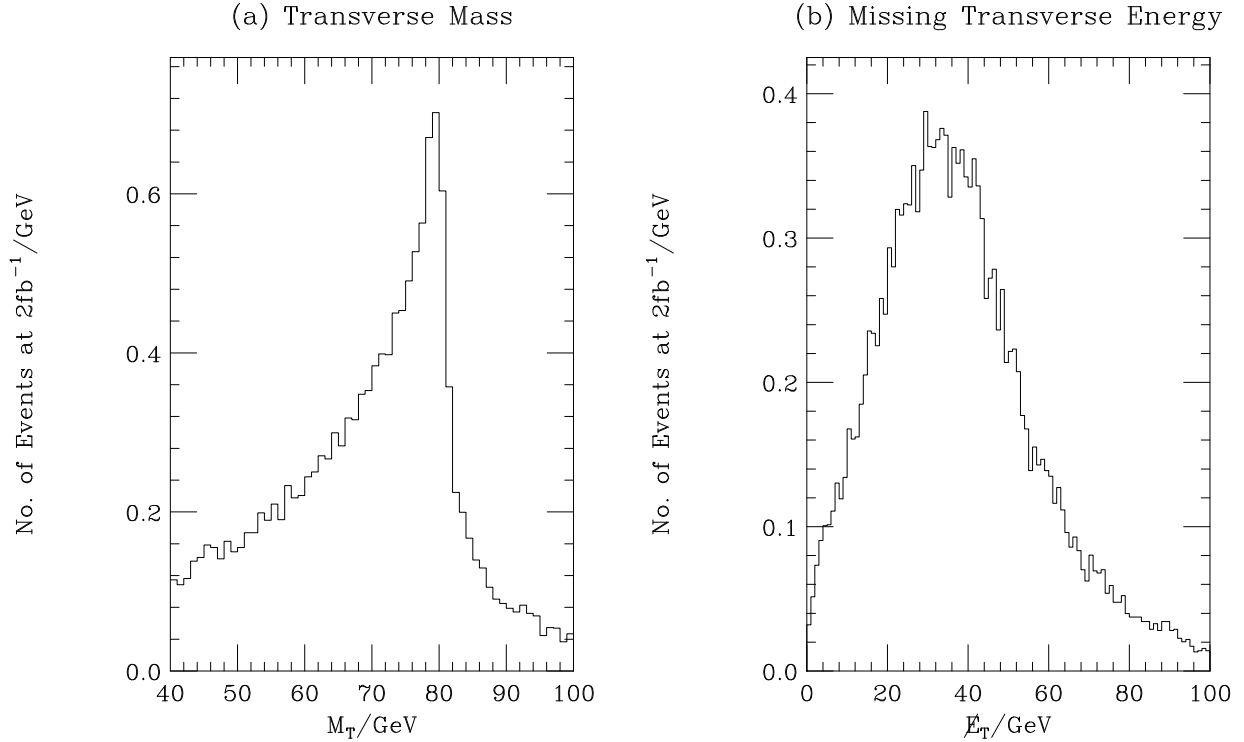


Figure 9: The transverse mass and missing transverse energy in WZ events at Run II of the Tevatron. The distributions are normalized to  $2 \text{ fb}^{-1}$  luminosity.

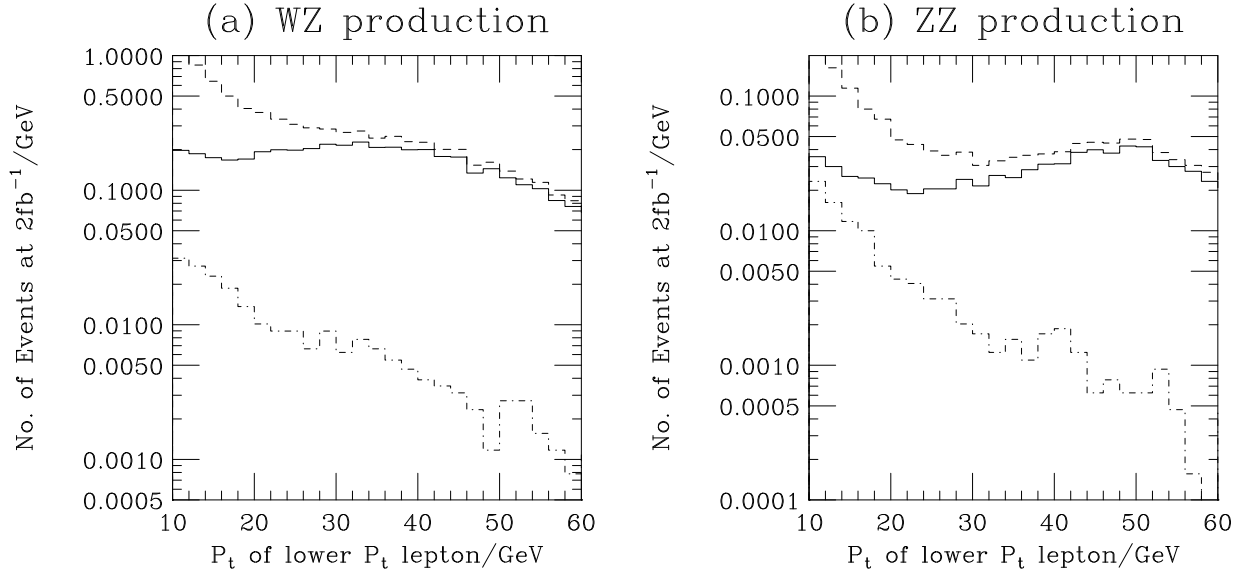


Figure 10: Effect of the isolation cuts on the WZ and ZZ backgrounds at Run II of the Tevatron. The dashed line gives the background before any cuts, the solid line shows the effect of the isolation cut described in the text. The dot-dash line gives the effect of all the cuts, including the cut on the number of jets. The distributions are normalized to  $2 \text{ fb}^{-1}$  luminosity.

pairs was imposed to reduce the background from Z production, rather than the veto on the presence of OSSF leptons which we have used. The veto and missing transverse energy cut will reduce the number of events from  $W\gamma$  production while the cut on the invariant mass will not suppress this background.

The effect of all these cuts on the background is given in Table 2. While the dominant background is from WZ production, the dominant contribution to the error comes from  $b\bar{b}$  production. This can only be reduced with a significantly more elaborate simulation.

We also need to calculate the acceptance of these cuts for the signal. To estimate the acceptance of the cuts we simulated twenty thousand events at one hundred points in the  $M_0, M_{1/2}$  plane. The acceptance was then interpolated between the points and multiplied by the cross section to give the number of signal events passing the cuts. This can then be used to find the discovery potential by comparing the number of signal events with a  $5\sigma$  statistical fluctuation of the background.

Fig. 11 shows the discovery potential, for different integrated luminosities and a fixed value of the coupling  $\lambda'_{211} = 10^{-2}$ , if we only consider the Standard Model backgrounds and apply the cuts we described to suppress these backgrounds. Fig. 12 shows the effect of varying the  $\mathcal{R}_p$  coupling for  $2 \text{ fb}^{-1}$  integrated luminosity with the same assumptions.

We have taken a conservative approach where the background is taken to be one standard deviation above the central value. Due to the small number of events we must use Poisson statistics, this means that for the Standard Model background given in Table 2, 7 events corresponds to the same probability as a  $5\sigma$  statistical fluctuation for a Gaussian distribution. Here we have used 0.59 events as a conservative estimate of the background, *i.e.* a  $1\sigma$  fluctuation above our central value.

For small couplings there are regions, for low  $M_{1/2}$ , which cannot be observed even for small smuon masses. For larger couplings however we can probe masses of up to 430 (500) GeV for a coupling  $\lambda'_{211} = 0.05$  with 2 (10)  $\text{fb}^{-1}$  integrated luminosity. Masses of up to 520 (600) GeV can be observed for a coupling of  $\lambda'_{211} = 0.1$  with 2 (10)  $\text{fb}^{-1}$  integrated luminosity.

We have neglected the non-physics background. This mainly comes from fake leptons in W production. The cuts we have applied to reduce the gauge boson pair production backgrounds, in particular the cuts on the missing transverse energy and the transverse mass, will significantly reduce this background. It was noted in [42] that the cross section falls extremely quickly with the  $p_T$  of the fake lepton, and hence the large  $p_T$  cut we have imposed will suppress this background. A proper treatment of the non-physics background requires a simulation of the detector. This is beyond the scope of this paper.

In Figs. 11 and 12 the background from sparticle pair production is neglected. This is reasonable in an initial search where presumably an experiment would be looking for an excess of like-sign dilepton pairs, rather than worrying about precisely which model was giving the excess. If such an excess were observed, it would then be necessary to establish which physical processes were producing the excess. In the  $\mathcal{R}_p$  MSSM there are two possible mechanisms which could produce such an excess: either resonant sparticle production; or sparticle pair production followed by the decay of the LSP. We will now consider additional cuts which will suppress the background to resonant slepton production

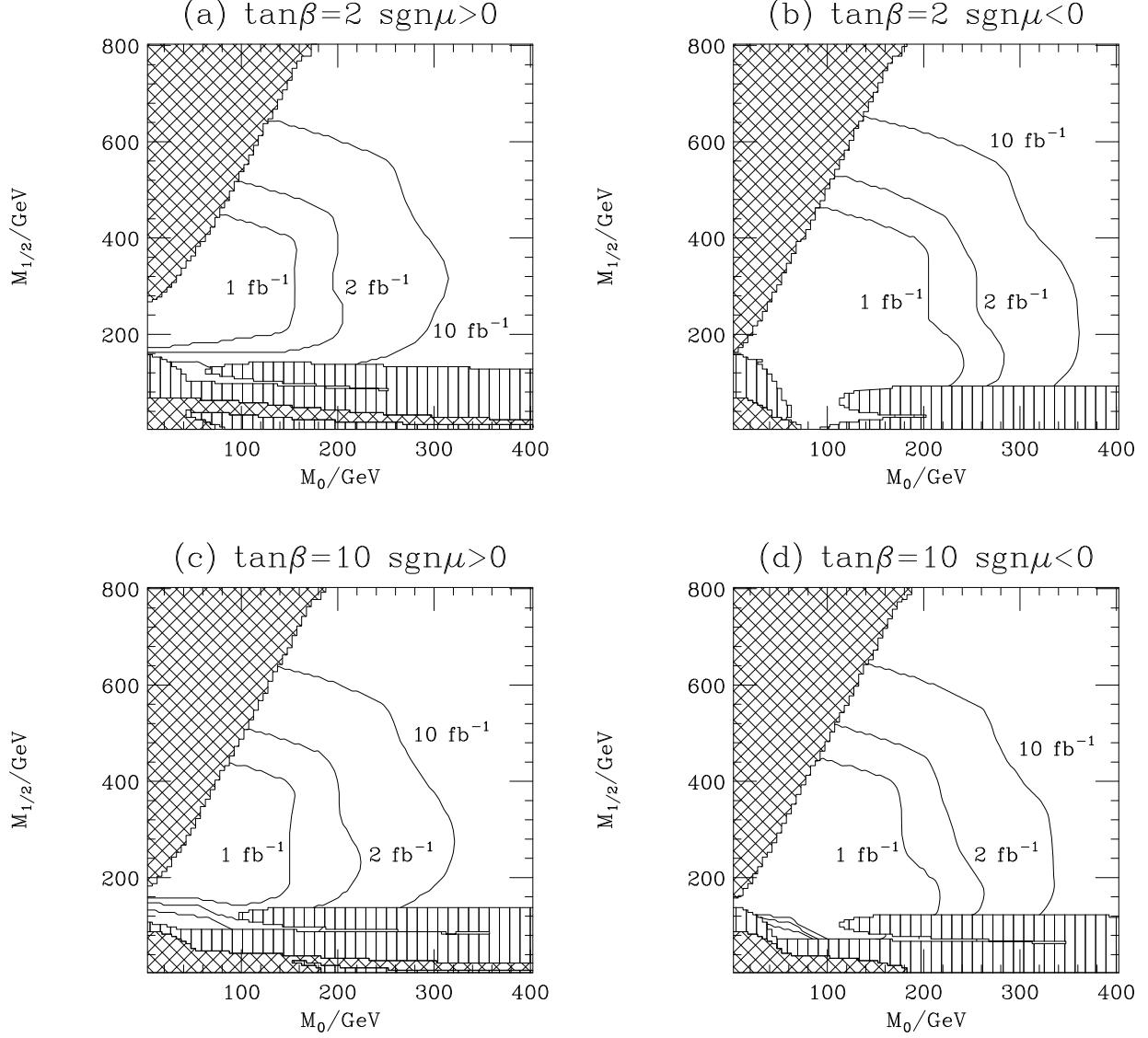


Figure 11: Contours showing the discovery potential of the Tevatron in the  $M_0$ ,  $M_{1/2}$  plane for  $\lambda'_{211} = 10^{-2}$  and  $A_0 = 0$  GeV. These are a  $5\sigma$  excess of the signal above the background. Here we have imposed the cuts on the isolation and  $p_T$  of the leptons, the transverse mass and the missing transverse energy described in the text, and a veto on the presence of OSSF leptons. We have only considered the Standard Model background. The striped and hatched regions are described in the caption of Fig. 3.

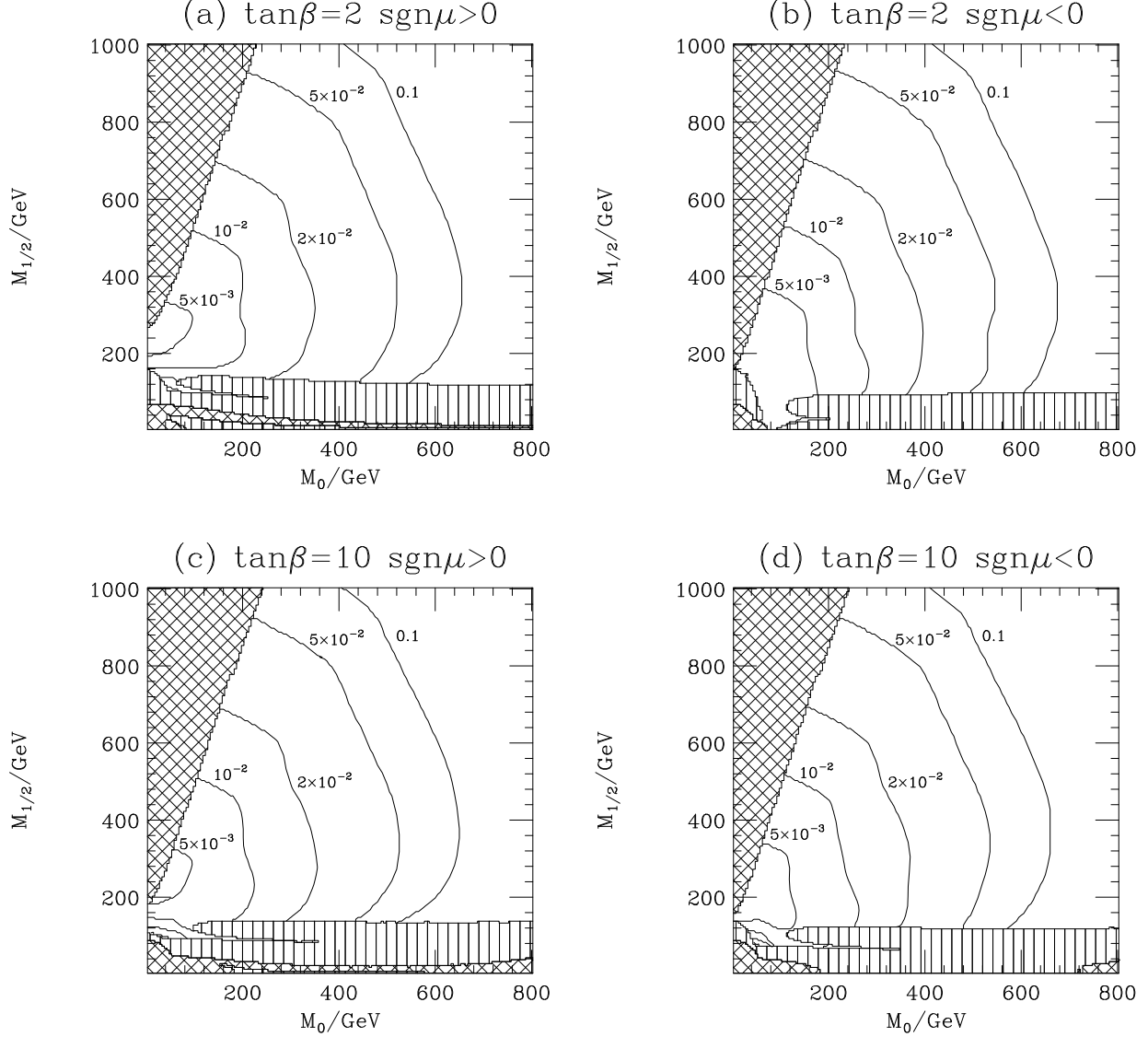


Figure 12: Contours showing the discovery potential of the Tevatron in the  $M_0$ ,  $M_{1/2}$  plane for  $A_0 = 0$  GeV and  $2 \text{ fb}^{-1}$  integrated luminosity for different values of  $\lambda'_{211}$ . These are a  $5\sigma$  excess of the signal above the background. Here we have imposed the cuts on the isolation and  $p_T$  of the leptons, the transverse mass and the missing transverse energy described in the text, and a veto on the presence of OSSF leptons. We have only considered the Standard Model background. The striped and hatched regions are described in the caption of Fig. 3.

from sparticle pair production and hopefully allow these two scenarios to be distinguished.

#### 4.1.2 SUSY backgrounds

We have seen that by imposing cuts on the transverse momentum and isolation of the like-sign dileptons, the missing transverse energy, the transverse mass and the presence of OSSF leptons the Standard Model backgrounds can be significantly reduced. However a significant background from sparticle pair production still remains. We therefore imposed the following additional cut to reduce this background:

- Vetoing all events when there are more than two jets each with  $p_T > 20$  GeV.

While this cut slightly reduces the signal it also dramatically reduces the background from sparticle pair production. We performed a scan of the SUGRA parameter space at the four values of  $\tan\beta$  and  $\text{sgn}\mu$  considered in Section 2. We generated fifty thousand events at each of one hundred points in the  $M_0, M_{1/2}$  plane at each value of  $\tan\beta$  and  $\text{sgn}\mu$ , and then interpolated between these points as for the signal process. This allowed us to estimate an acceptance for the cuts which we multiplied by the sparticle pair production cross section to give a number of background events.

The effect of all the cuts on the total background, *i.e.* the Standard Model background and the sparticle pair production background is shown in Fig. 13 for different integrated luminosities with  $\lambda'_{211} = 10^{-2}$  and in Fig. 14 for an integrated luminosity of  $2 \text{ fb}^{-1}$  with different values of  $\lambda'_{211}$ .

As can be seen, the effect of including the sparticle pair production background is to reduce the  $5\sigma$  discovery regions. These regions are reduced for two reasons: for large  $M_{1/2}$  the additional cut removes more signal events and hence reduces the statistical significance of the signal; at small values of  $M_{1/2}$  there is a large background from sparticle pair production, relative to the SM background, which also reduces the statistical significance of the signal. However even for this relatively small value of the coupling there are large regions of parameter space in which a signal is visible above the background. The ratio of signal to background is still larger than one for most of the region where the signal is detectable above the background. For  $\text{sgn}\mu > 0$  there is only a very small region at low  $M_{1/2}$  where  $S/B$  drops below one and even here  $S/B > 0.5$ . However for  $\text{sgn}\mu < 0$  there are regions of low  $S/B$  for small values of  $M_{1/2}$ . The discovery range for these  $\mathcal{R}_p$  processes extends to larger values of  $M_{1/2}$  than the  $5\sigma$  discovery curve for sparticle pair production as only one sparticle is produced which requires a much lower parton-parton centre-of-mass energy than sparticle pair production.

Again even for small smuon masses with low values of the  $\mathcal{R}_p$  Yukawa coupling there are regions where a signal of resonant slepton production is not visible above the background. However for large couplings the signal in these regions is visible above the background. For a coupling of  $\lambda'_{211} = 0.05$  a smuon mass of 310 (330) GeV is visible above the background with  $2$  ( $10$ )  $\text{fb}^{-1}$  integrated luminosity, and for a coupling of  $\lambda'_{211} = 0.1$  a smuon mass of 400 (430) GeV is visible above the background with  $2$  ( $10$ )  $\text{fb}^{-1}$  integrated luminosity.

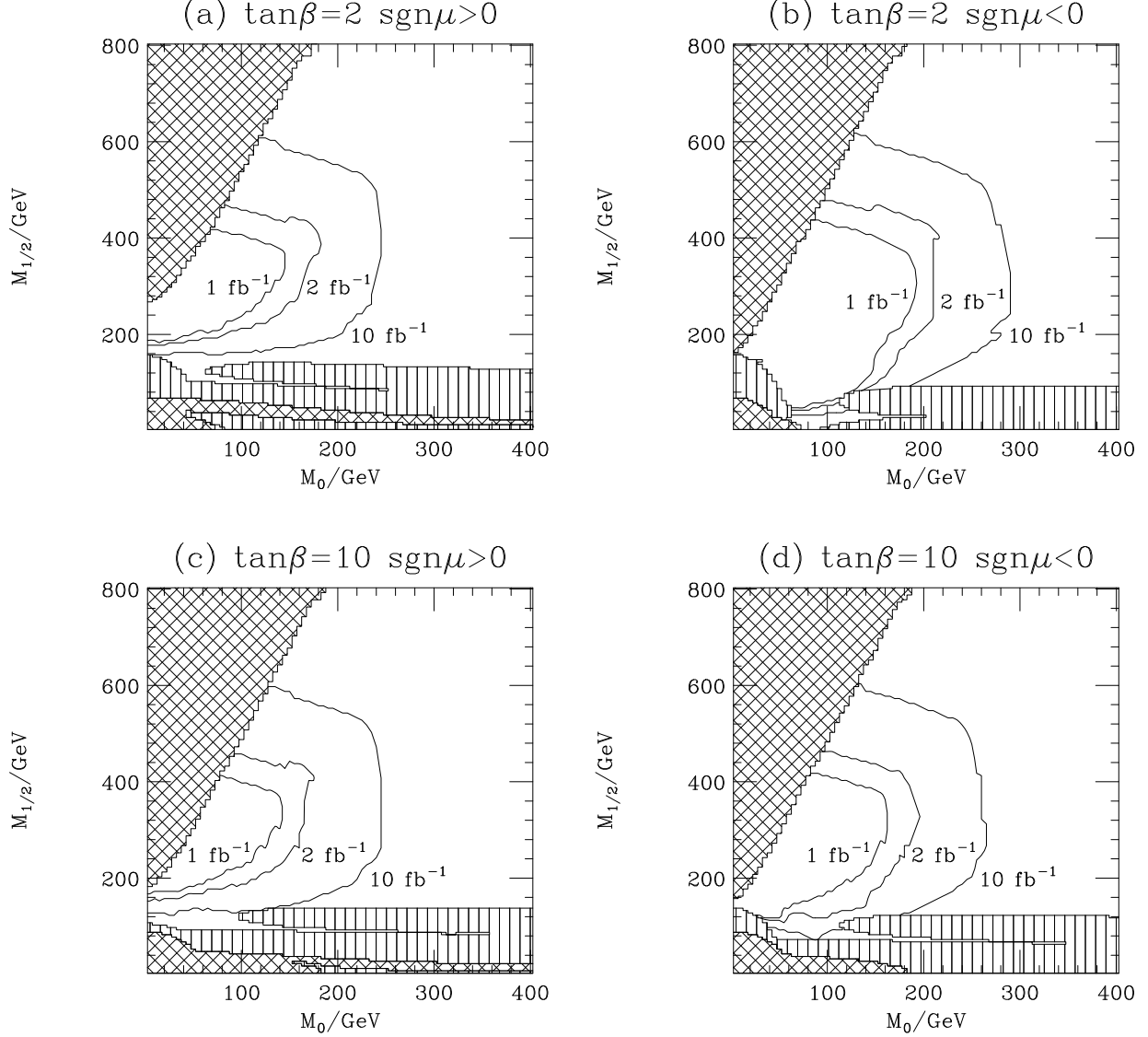


Figure 13: Contours showing the discovery potential of the Tevatron in the  $M_0$ ,  $M_{1/2}$  plane for  $\lambda'_{211} = 10^{-2}$  and  $A_0 = 0$  GeV. These are a  $5\sigma$  excess of the signal above the background. Here in addition to the cuts on the isolation and  $p_T$  of the leptons, the transverse mass and the missing transverse energy described in the text, and a veto on the presence of OSSF leptons we have imposed a cut on the presence of more than two jets. This includes the sparticle pair production background as well as the Standard Model backgrounds. Again the striped and hatched regions are as described in the caption of Fig. 3.



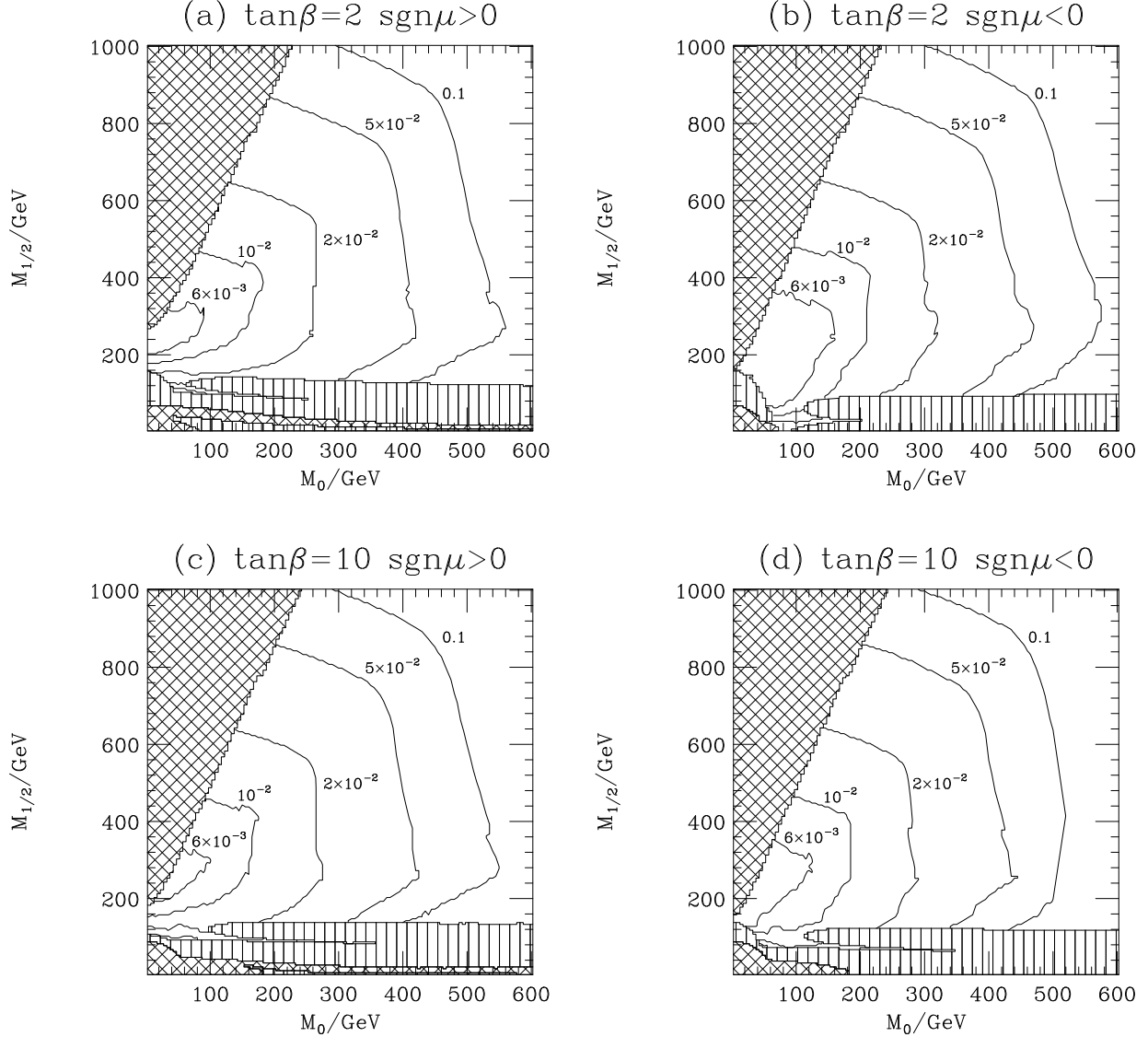


Figure 14: Contours showing the discovery potential of the Tevatron in the  $M_0$ ,  $M_{1/2}$  plane for  $A_0 = 0$  GeV and an integrated luminosity of  $2 \text{ fb}^{-1}$  for different values of  $\lambda'_{211}$ . These are a  $5\sigma$  excess of the signal above the background. Here in addition to the cuts on the isolation and  $p_T$  of the leptons, the transverse mass and the missing transverse energy described in the text, and a veto on the presence of OSSF leptons we have imposed a cut on the presence of more than two jets. This includes the sparticle pair production background as well as the Standard Model backgrounds. Again the striped and hatched regions are as described in the caption of Fig. 3.

## 4.2 LHC

The cross section for the production of a charged lepton and a neutralino, which is again the dominant production mechanism, at the LHC is shown in Fig. 15 in the  $M_0, M_{1/2}$  plane with  $A_0 = 0$  GeV and  $\lambda'_{211} = 10^{-2}$  for two different values of  $\tan \beta$  and both values of  $\text{sgn } \mu$ . The total cross section for resonant slepton production followed by a supersymmetric gauge decay is shown in Fig. 16. As for the Tevatron, the total resonant slepton cross section closely follows the slepton mass contours whereas the cross section for neutralino lepton production falls-off more quickly at small  $M_{1/2}$  because the branching ratio for  $\tilde{\mu}_L \rightarrow \mu \tilde{\chi}_1^0$  is reduced due to the production of charginos and the heavier neutralinos. We adopted the same procedure described in Section 4.1 to estimate the acceptance of the cuts we have imposed. We will again first consider the cuts required to reduce the Standard Model backgrounds and then the additional cut used to suppress the sparticle pair production background.

### 4.2.1 Standard Model Backgrounds

We applied the following cuts to reduce the Standard Model backgrounds:

1. A cut requiring all the leptons to be in the central region of the detector  $|\eta| < 2.0$ .
2. A cut on the transverse momentum of the like-sign leptons  $p_T^{\text{lepton}} \geq 40$  GeV, this is the lowest cut we could apply given our parton-level cut of  $p_T^{\text{parton}} = 40$  GeV, for the  $b\bar{b}$  background.
3. An isolation cut on the like-sign leptons so that the transverse energy in a cone of radius,  $R = \sqrt{\Delta\phi^2 + \Delta\eta^2} = 0.4$ , about the direction of the lepton is less than 5 GeV.
4. We reject events with  $60 \text{ GeV} < M_T < 85 \text{ GeV}$  (*c.f.* Eqn. 8.) This cut is applied to both of the like-sign leptons.
5. A veto on the presence of a lepton in the event with the same flavour but opposite charge as either of the leptons in the like-sign pair if the lepton has  $p_T > 10$  GeV and passes the same isolation cut as the like-sign leptons.
6. A cut on the missing transverse energy,  $\cancel{E}_T < 20$  GeV.

The first two cuts are designed to reduce the background from heavy quark, *i.e.*  $b\bar{b}$  and  $t\bar{t}$  production which is again the major source of backgrounds before any cuts. However, as can be seen in Fig. 17, after the imposition of the  $p_T$  and isolation cuts this background is significantly reduced. It remains the major source of the error on the background however due to the large cross section for  $b\bar{b}$  production which makes it impossible to simulate the full luminosity of the LHC with the resources available.

The remaining cuts reduce the background from gauge boson pair, particularly WZ, production which dominates the Standard Model background after the imposition of the isolation and  $p_T$  cuts. Fig. 18a shows that the cut on the transverse mass, *i.e.* removing the

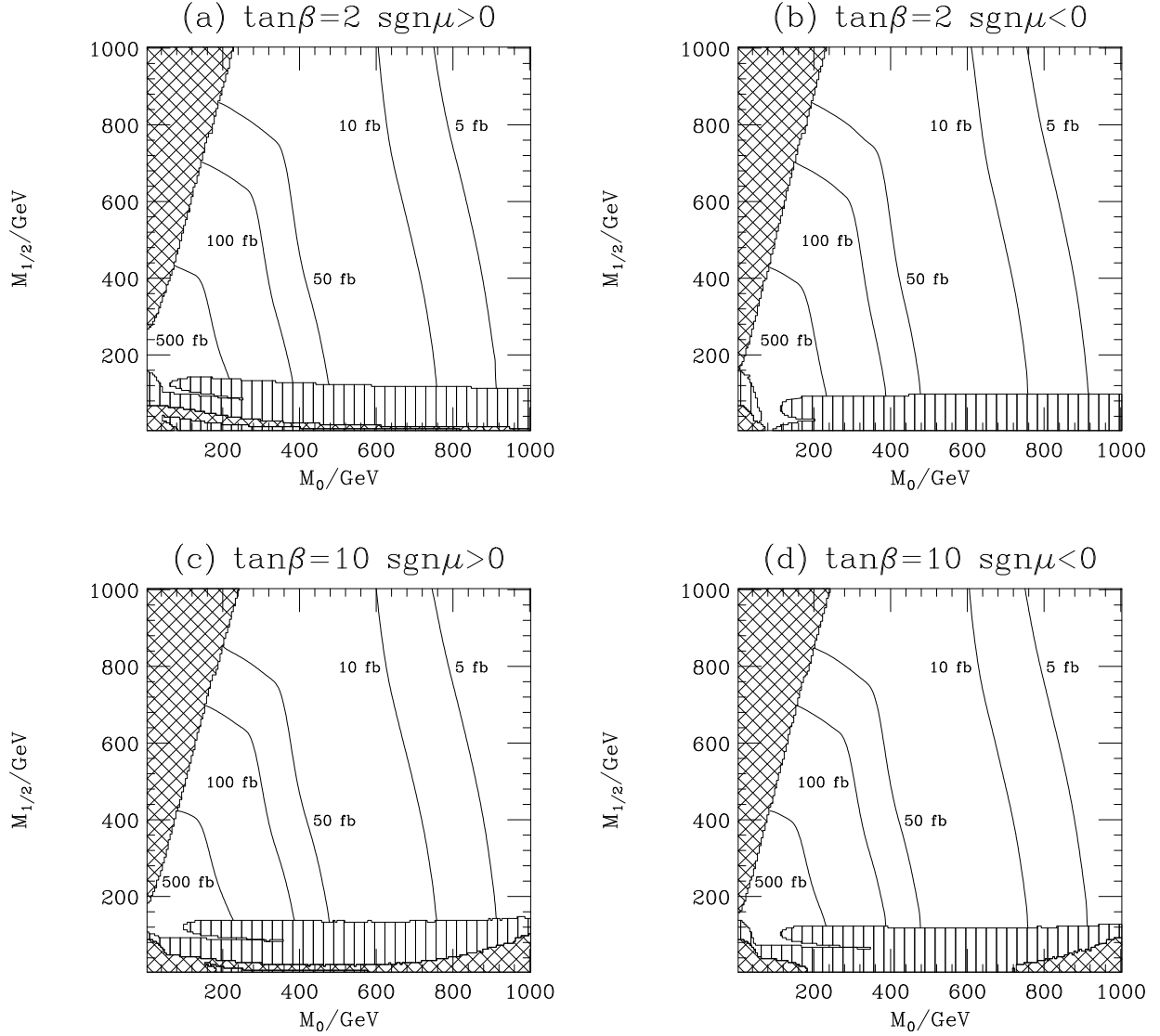


Figure 15: Contours showing the cross section for the production of a neutralino and a charged lepton at the LHC in the  $M_0, M_{1/2}$  plane for  $A_0 = 0$  GeV and  $\lambda'_{211} = 10^{-2}$  with different values of  $\tan\beta$  and  $\text{sgn}\mu$ . The striped and hatched regions are described in the caption of Fig. 3.

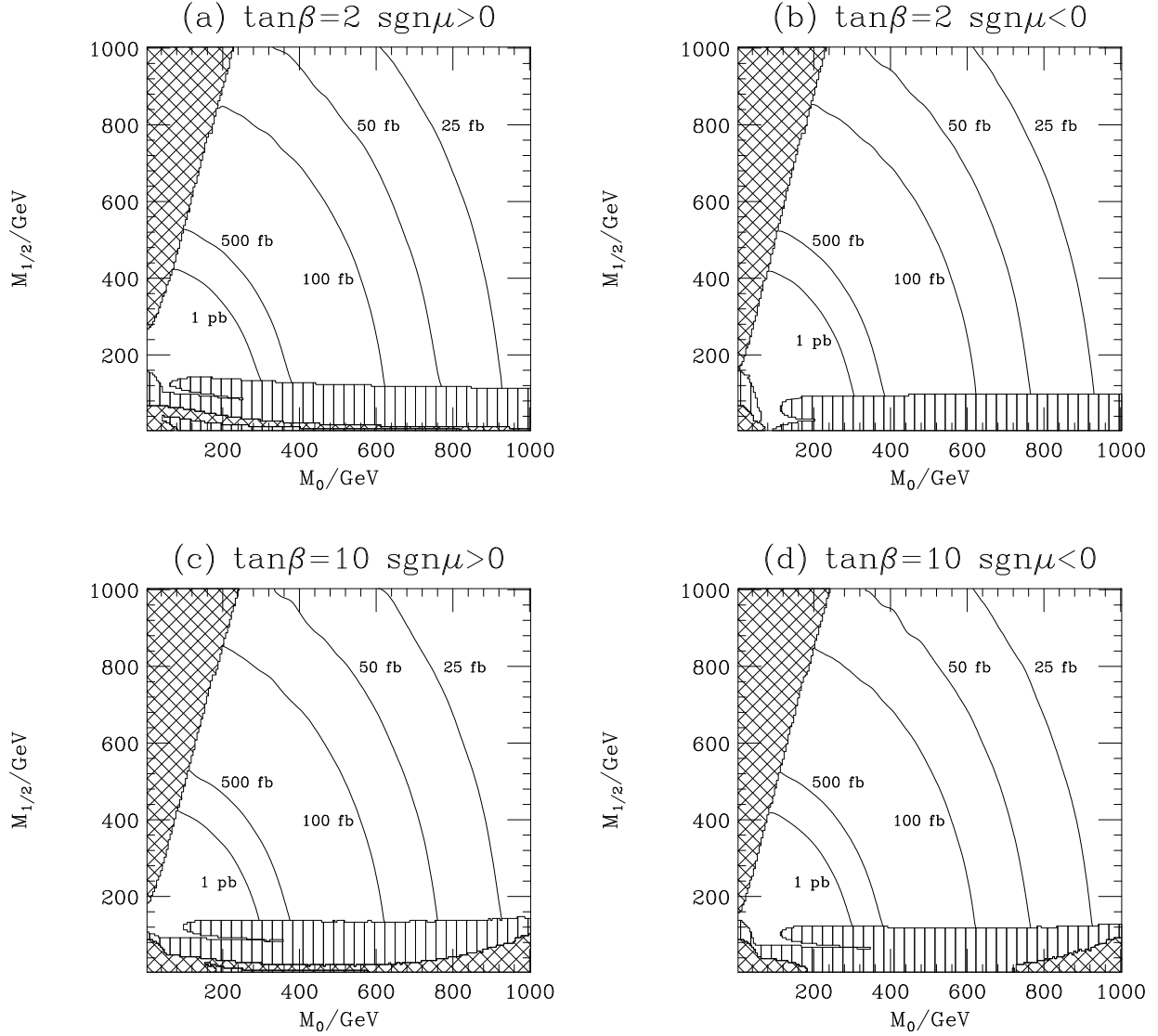


Figure 16: Contours showing the cross section for resonant slepton production followed by a supersymmetric gauge decay at the LHC in the  $M_0, M_{1/2}$  plane for  $A_0 = 0$  GeV and  $\lambda'_{211} = 10^{-2}$  with different values of  $\tan\beta$  and  $\text{sgn}\mu$ . The striped and hatched regions are described in the caption of Fig. 3.

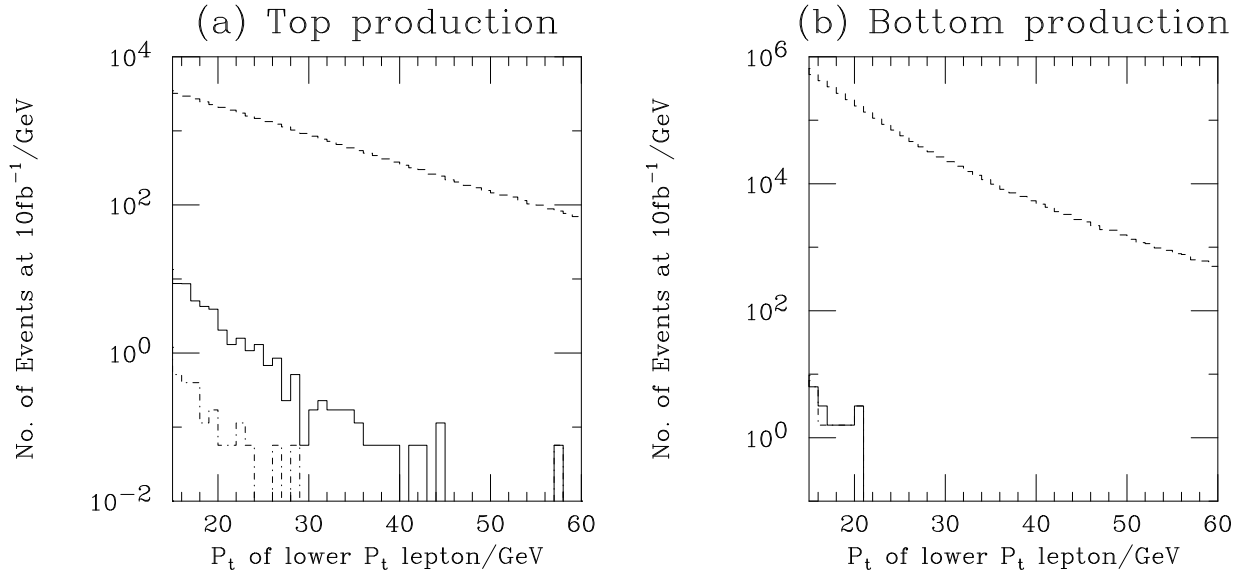


Figure 17: Effect of the isolation cuts on the  $t\bar{t}$  and  $b\bar{b}$  backgrounds at the LHC. The dashed line gives the background before any cuts, the solid line shows the effect of the isolation cut described in the text. The dot-dash line gives the effect of all the cuts, including the cut on the number of jets, for the  $b\bar{b}$  background this is almost indistinguishable from the solid line. As a parton-level cut of 40 GeV was used in simulating the  $b\bar{b}$  background the results below 40 GeV for the lepton  $p_T$  do not correspond to the full number of background events. The distributions have been normalized to  $10 \text{ fb}^{-1}$  integrated luminosity.

region  $60 \text{ GeV} < M_T < 85 \text{ GeV}$ , for each of the like sign leptons will reduce the background from WZ production, which is the largest of the gauge boson pair production backgrounds. Similarly the cut on the missing transverse energy,  $\cancel{E}_T < 20 \text{ GeV}$ , will significantly reduce the background from WZ production as can be seen in Fig. 18b. The effect of these cuts is shown in Fig. 19. Again the simulation of the gauge boson pair production backgrounds does not include  $W\gamma$  production which may be an important source of background, but should be significantly reduced by the cuts.

The effect of all these cuts on the background is shown in Table 3. While the dominant background is from WZ production, the dominant contribution to the error comes from  $b\bar{b}$  production. This can only be reduced with a significantly more elaborate simulation.

This gives a total background after all the cuts of  $4.9 \pm 1.6$  events, for  $10 \text{ fb}^{-1}$  integrated luminosity. If we take a conservative approach and take a background of 6.5 events, *i.e.* a  $1\sigma$  fluctuation above the central value of our calculation a  $5\sigma$  statistical fluctuation would correspond to 16 events, for an integrated luminosity of  $10 \text{ fb}^{-1}$ . As can be seen from Fig. 17 this is a conservative upper bound.

We adopted the same procedure described in the previous section to obtain the acceptance for the  $\mathcal{R}_p$  signal given the cuts we have imposed. The discovery potential of the LHC is shown in Fig. 20, for  $\lambda'_{211} = 10^{-2}$  with different integrated luminosities, and

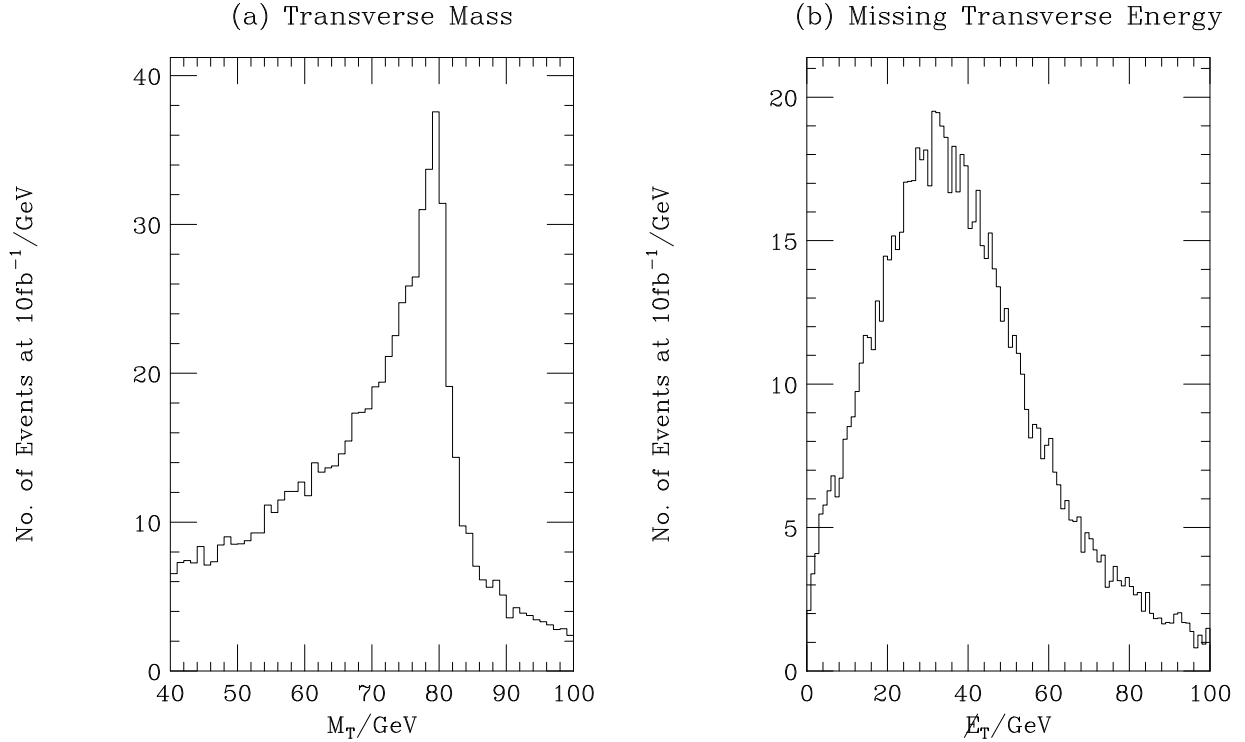


Figure 18: The transverse mass and missing transverse energy in WZ events at the LHC. The distributions are normalized to  $10 \text{ fb}^{-1}$  luminosity.

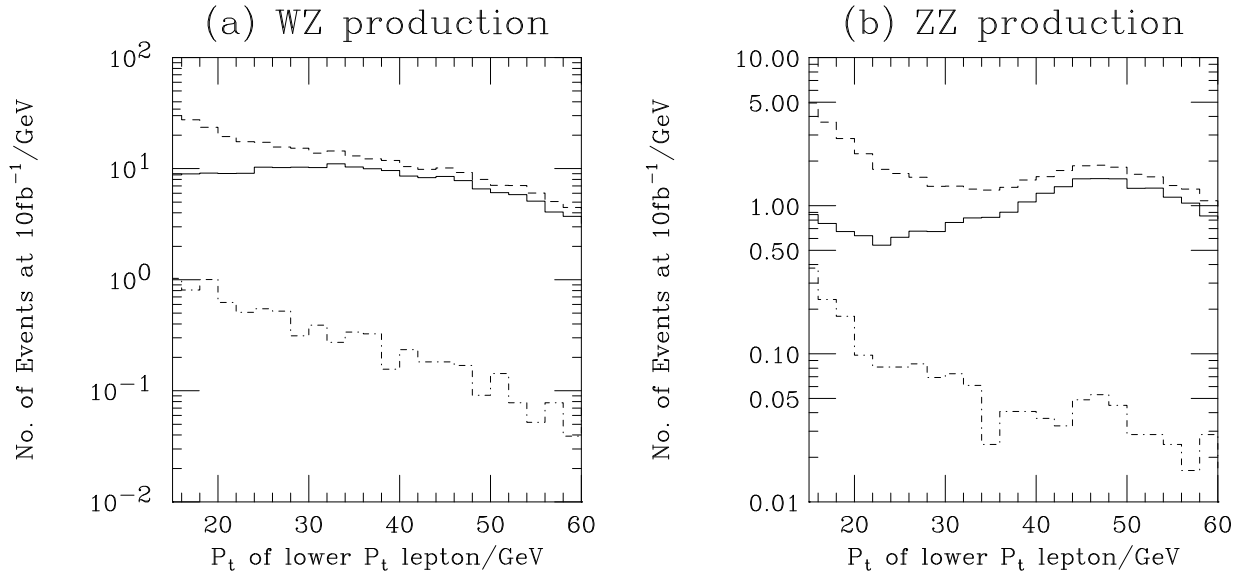


Figure 19: Effect of the isolation cuts on the WZ and ZZ backgrounds at the LHC. The dashed line gives the background before any cuts, the solid line shows the effect of the isolation cut described in the text. The dot-dash line gives the effect of all the cuts, including the cut on the number of jets. The distributions are normalized to  $10 \text{ fb}^{-1}$  luminosity.

Background Process	Number of Events			
	After $p_T$ cut	After isolation and $p_T$ cuts	After isolation, $p_T$ , $M_T$ , $\cancel{E}_T$ cuts and OSSF lepton veto.	After all cuts
WW	$3.6 \pm 0.5$	$0.0 \pm 0.06$	$0.0 \pm 0.06$	$0.0 \pm 0.06$
WZ	$239 \pm 2.5$	$198.6 \pm 2.3$	$3.8 \pm 0.3$	$3.8 \pm 0.3$
ZZ	$55.4 \pm 0.7$	$45.2 \pm 0.6$	$1.04 \pm 0.09$	$1.04 \pm 0.09$
$t\bar{t}$	$(4.4 \pm 0.2) \times 10^3$	$0.28 \pm 0.13$	$0.06 \pm 0.06$	$0.06 \pm 0.06$
bb	$(4.4 \pm 0.9) \times 10^4$	$0.0 \pm 1.6$	$0.0 \pm 1.6$	$0.0 \pm 1.6$
Single Top	$36.6 \pm 1.5$	$0.0 \pm 0.004$	$0.0 \pm 0.004$	$0.0 \pm 0.004$
Total	$(4.9 \pm 0.9) \times 10^4$	$244.1 \pm 2.9$	$4.9 \pm 1.6$	$4.9 \pm 1.6$

Table 3: Backgrounds to like-sign dilepton production at the LHC. The numbers of events are based on an integrated luminosity of  $10 \text{ fb}^{-1}$ . Again we have calculated an error on the cross section by varying the scale between half and twice the hard scale, apart from the gauge boson pair cross section where we do not have this information and the effect of varying the scale is expected to be small anyway. The error on the number of events is then the error on the cross section and the statistical error from the Monte Carlo simulation added in quadrature. If no events passed the cut the statistical error was taken to be the same as if one event had passed the cuts.

in Fig. 21, for an integrated luminosity of  $10 \text{ fb}^{-1}$  with different values of  $\lambda'_{211}$ . This is considerably greater than the discovery potential of the Tevatron at high  $M_0$  and  $M_{1/2}$  due to the larger centre-of-mass energy of the LHC and hence the larger cross sections. In particular the search potential with one years running at high luminosity, *i.e.*  $100 \text{ fb}^{-1}$ , covers large regions of the  $M_0$ ,  $M_{1/2}$  plane. At very large values of  $M_{1/2}$  this extends to regions where the sparticle pair production cross section is small due to the high masses of the SUSY particles.

At small values of  $M_0$  and  $M_{1/2}$  there are regions of SUGRA parameter space which cannot be probed for any couplings due to the cuts we have applied. However these regions can be excluded by either LEP or the Tevatron and we will therefore ignore them in the rest of this analysis. If we neglect these regions the LHC can observe a resonant slepton with a mass of up to 510 (710) GeV for a coupling of  $\lambda'_{211} = 0.02$  with  $10$  ( $100$ )  $\text{fb}^{-1}$  integrated luminosity and for a coupling  $\lambda'_{211} = 0.05$  a resonant slepton can be observed with a mass of 750 (950) GeV with  $10$  ( $100$ )  $\text{fb}^{-1}$  integrated luminosity.

As with the Tevatron analysis we have neglected the background from sparticle pair production which is reasonable in an initial search for an excess of like-sign dilepton pairs over the Standard Model expectation. If such an excess were observed it would then be necessary to establish which process was producing the effect. In the next section, we will present the cuts necessary to reduce the background from sparticle pair production and

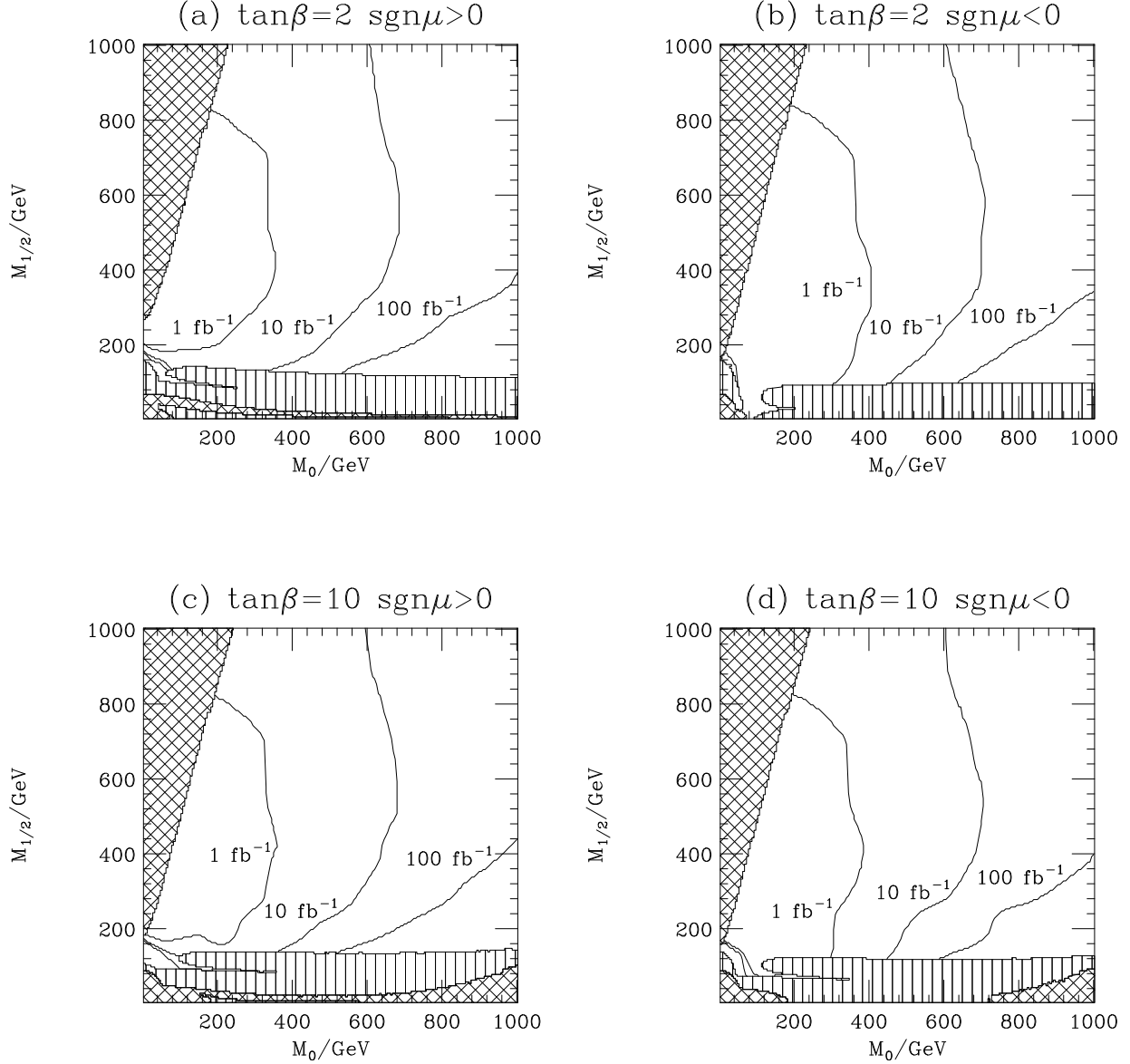


Figure 20: Contours showing the discovery potential of the LHC in the  $M_0$ ,  $M_{1/2}$  plane for  $\lambda'_{211} = 10^{-2}$  and  $A_0 = 0$  GeV. These are a  $5\sigma$  excess of the signal above the background. Here we have imposed cuts on the isolation and  $p_T$  of the leptons, the transverse mass and the missing transverse energy described in the text, and a veto on the presence of OSSF leptons. We have only considered the Standard Model background. The striped and hatched regions are described in the caption of Fig. 3.



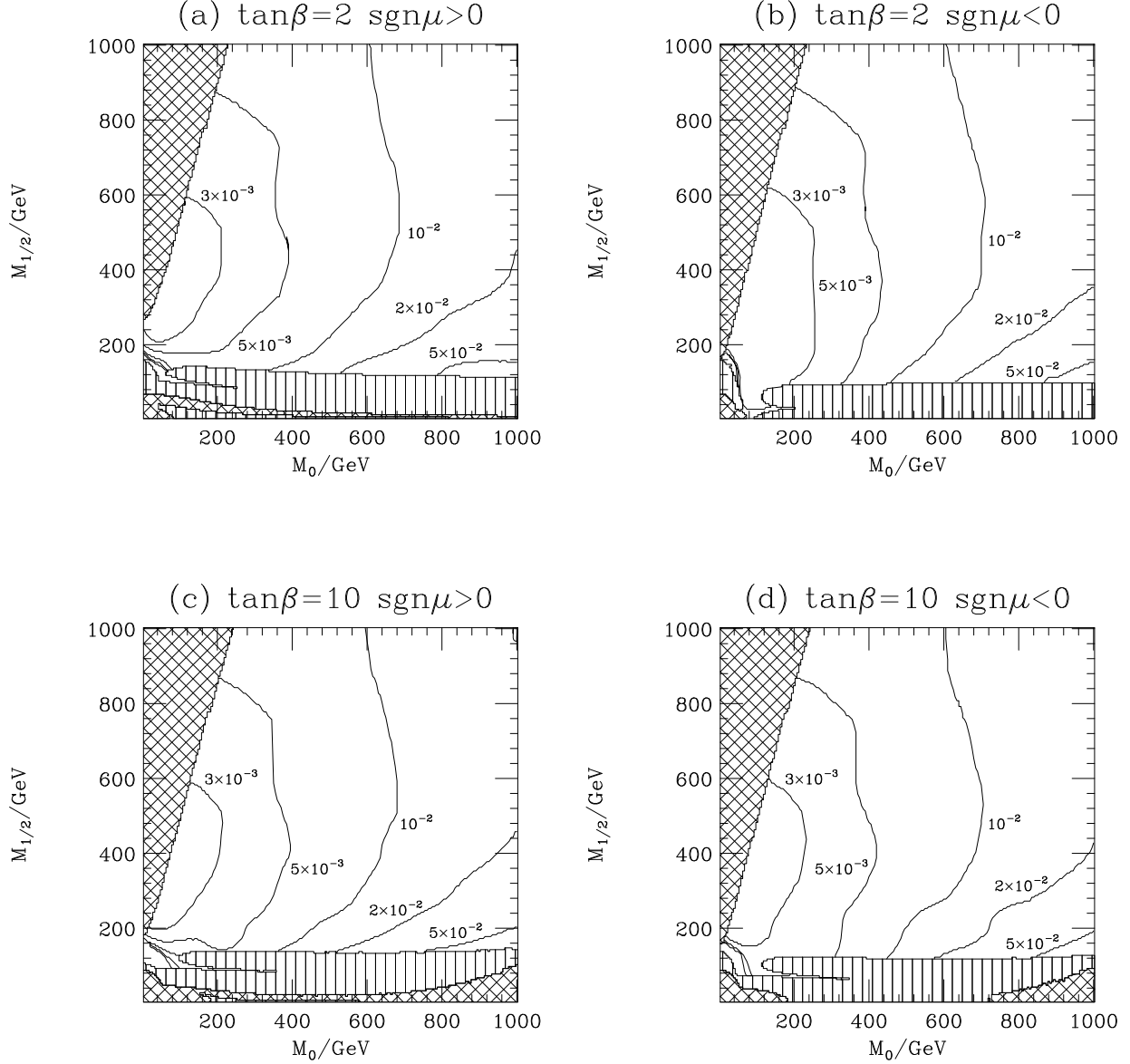


Figure 21: Contours showing the discovery potential of the LHC in the  $M_0$ ,  $M_{1/2}$  plane for  $A_0 = 0$  GeV and an integrated luminosity of  $10 \text{ fb}^{-1}$  with different values of  $\lambda'_{211}$ . These are a  $5\sigma$  excess of the signal above the background. Here we have imposed cuts on the isolation and  $p_T$  of the leptons, the transverse mass and the missing transverse energy described in the text, and a veto on the presence of OSSF leptons. We have only considered the Standard Model background. The striped and hatched regions are described in the caption of Fig. 3.

enable a resonant slepton signature to be established over all the backgrounds.

### 4.2.2 SUSY backgrounds

The background from sparticle pair production is much more important at the LHC than the Tevatron given the much higher cross sections for sparticle pair production. The nature of the sparticles produced is also different due to the higher energies. In the regions of SUGRA parameter space where the pair production cross section at the Tevatron is large the lightest SUSY particles, *i.e.* the electroweak gauginos, are predominately produced. This is because the production of the heavier squarks and gluinos is suppressed by the higher parton-parton centre-of-mass energies required. However given the higher centre-of-mass energy of the LHC the production of the coloured sparticles which occurs via the strong interaction dominates the cross section. This means that a cut on the number of jets in an event will be more effective in reducing the background from sparticle pair production. The following cut was applied:

- Vetoing all events when there are more than two jets each with  $p_T > 50$  GeV.

As the sparticle pair production background at the LHC is larger than at the Tevatron we needed to simulate more events in order to obtain a reliable estimate of the acceptance for this background. This meant that with the available resources we were forced to use a coarser scan of the  $M_0$ ,  $M_{1/2}$  plane. We used a 16 point grid and simulated a different number of events at each point depending on the value of  $M_{1/2}$  as the sparticle pair production cross section is decreases as  $M_{1/2}$  increases. We simulated  $10^5$ ,  $10^5$ ,  $10^6$ , and  $10^7$  events at each of four points for  $M_{1/2} = 875$  GeV,  $M_{1/2} = 625$  GeV,  $M_{1/2} = 375$  GeV and  $M_{1/2} = 125$  GeV, respectively.

Our estimate of the discovery potential of the LHC after this cut, including all the backgrounds is given in Fig. 22, for  $\lambda_{211} = 10^{-2}$  with different integrated luminosities, and in Fig. 23, for an integrated luminosity of  $10 \text{ fb}^{-1}$  with different values of the  $\mathcal{R}_p$  Yukawa couplings. As with the Tevatron the discovery potential is reduced in two regions relative to that shown in Figs. 20 and 21. The reduction at high  $M_{1/2}$  is due to the smaller signal after the imposition of the jet cut, whereas the reduction at small  $M_{1/2}$  is due to the larger background. However there are still large regions of SUGRA parameter space in which this process is visible above the background, particularly at large  $M_{1/2}$  where there is less sensitivity to sparticle pair production. Due to the larger backgrounds from sparticle pair production there are large regions where the signal is detectable above the background although the  $S/B$  is small. In general there is a region extending around 200 GeV in  $M_{1/2}$  above the bottom of the  $5\sigma$  discovery contour for  $100 \text{ fb}^{-1}$  where  $S/B < 1$ .

If we again neglect the region at small  $M_0$  and  $M_{1/2}$ , which cannot be probed for any  $\mathcal{R}_p$  Yukawa couplings given our cuts, we can obtain a mass reach for the LHC, with a given  $\mathcal{R}_p$  Yukawa coupling. Slepton masses of 460 (600) GeV can be discovered with  $10$  ( $100$ )  $\text{fb}^{-1}$  integrated luminosity for a coupling  $\lambda'_{211} = 0.05$  and slepton masses of 610 (820) GeV can be observed with  $10$  ( $100$ )  $\text{fb}^{-1}$  integrated luminosity for a coupling  $\lambda'_{211} = 0.1$ .

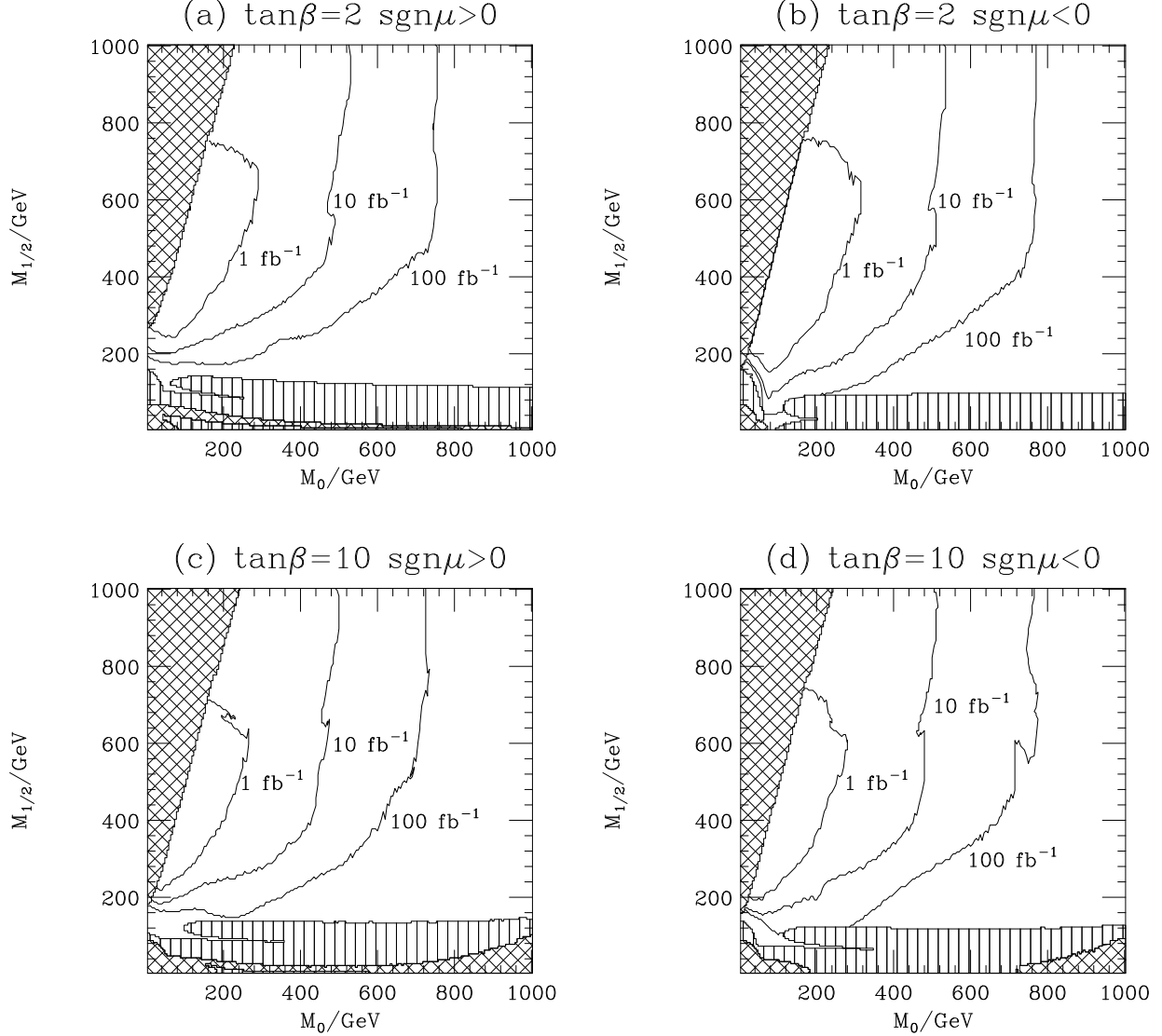


Figure 22: Contours showing the discovery potential of the LHC in the  $M_0$ ,  $M_{1/2}$  plane for  $\lambda'_{211} = 10^{-2}$  and  $A_0 = 0$  GeV. These are a  $5\sigma$  excess of the signal above the background. Here in addition to the cuts on the isolation and  $p_T$  of the leptons, the transverse mass and the missing transverse energy described in the text, and a veto on the presence of OSSF leptons we have imposed a cut on the presence of more than two jets. Here we have included the sparticle pair production background as well as the Standard Model backgrounds. The striped and hatched regions are described in the caption of Fig. 3.

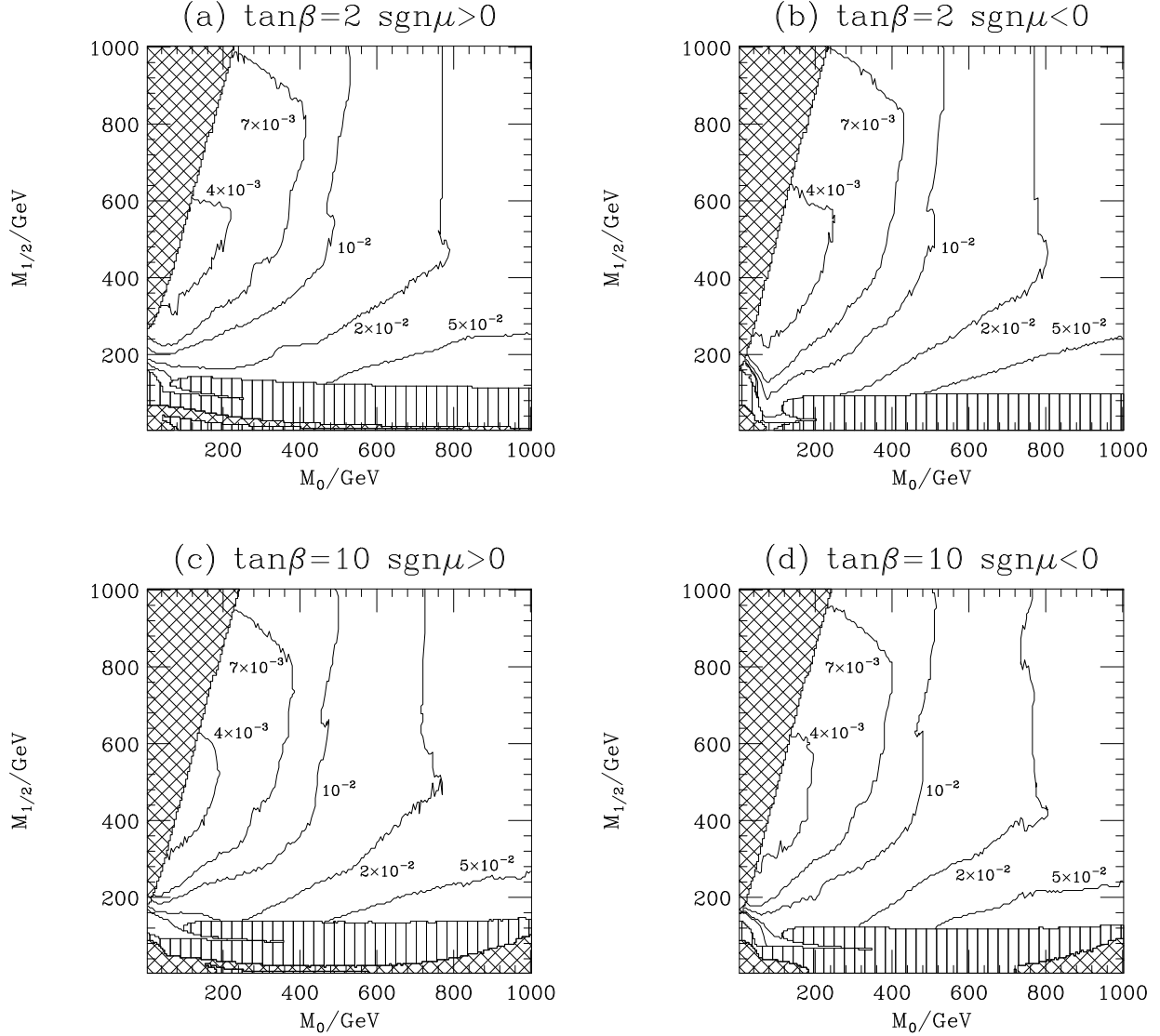


Figure 23: Contours showing the discovery potential of the LHC in the  $M_0$ ,  $M_{1/2}$  plane for  $A_0 = 0$  GeV and an integrated luminosity of  $10 \text{ fb}^{-1}$  with different values of  $\lambda'_{211}$ . These are a  $5\sigma$  excess of the signal above the background. Here in addition to the cuts on the isolation and  $p_T$  of the leptons, the transverse mass and the missing transverse energy described in the text, and a veto on the presence of OSSF leptons we have imposed a cut on the presence of more than two jets. Here we have included the sparticle pair production background as well as the Standard Model backgrounds. The striped and hatched regions are described in the caption of Fig. 3.

### 4.3 Mass Reconstruction

There are many possible models which lead to an excess of like-sign dilepton pairs, over the prediction of the Standard Model. Indeed, we have seen that within the  $\mathcal{R}_p$  extension of the MSSM such an excess could be due to either sparticle pair production followed by  $\mathcal{R}_p$  decays of the LSPs, or resonant charged slepton production followed by a supersymmetric gauge decay of the slepton. The cut on the number of jets described above gives one way of discriminating between these two scenarios.

An additional method of distinguishing between these two scenarios is to try and reconstruct the masses of the decaying sparticles for the resonant slepton production. In principle this is straightforward. The neutralino decay to a quark-antiquark pair and a charged lepton, will give two jets (or more after the emission of QCD radiation) and a charged lepton. These decay products should be relatively close together. Therefore to reconstruct the neutralino we took the highest two  $p_T$  jets in the event and combined them with the charged lepton which was closest in  $(\eta, \phi)$  space. We only used events in which both jets had  $p_T > 10$  GeV in addition to passing all the cuts described, *i.e.* both the cuts required to suppress the Standard Model and SUSY backgrounds, in the previous sections. This then gives a neutralino candidate, the masses of these candidates are shown for a sample point in SUSY parameter space for both the Tevatron, Fig. 24, and the LHC, Fig. 25. In both cases in addition to showing the result for the coupling  $\lambda'_{211} = 10^{-2}$ , we have shown a coupling such that the signal is exactly  $5\sigma$  above the background at this point to show what can be seen if the signal is only just detectable. As can be seen in both figures the reconstructed neutralino mass is in good agreement with the simulated value, although the situation may be worse once detector effects have been included.

We can then combine this neutralino candidate with the remaining lepton in the event to give a slepton candidate, under the assumption that the like-sign leptons were produced in the process  $\tilde{\ell}^+ \rightarrow \ell^+ \tilde{\chi}_1^0$ . The mass distribution of these slepton candidates is shown in Fig. 26 for the Tevatron and Fig. 27 for the LHC. Again there is good agreement between the position of the peak in the distribution and the value of the smuon mass used in the simulation.

The data for both the neutralino and smuon mass reconstructions is binned in 10 GeV bins. We have used the events in the central bin and the two bins on either side to reconstruct the neutralino and smuon masses. These reconstructed masses are given in Table 4. As can be seen for both the points we have shown the reconstructed mass lies between 5 GeV and 15 GeV below the simulated sparticle mass. This is due to the loss of some of the energy of the jets produced in the neutralino decay from the cones used to define the jets. It is common to include this effect in the jet energy correction, so this shift would probably not be observed in a full experimental simulation.

The agreement between the results of the simulation and the input values is good provided that the Standard Model background is dominant over the background from sparticle pair production and the lightest neutralino is predominantly produced in the smuon decay. This is the case at the points used in Figs. 24-27. At the point  $M_0 = 50$  GeV,

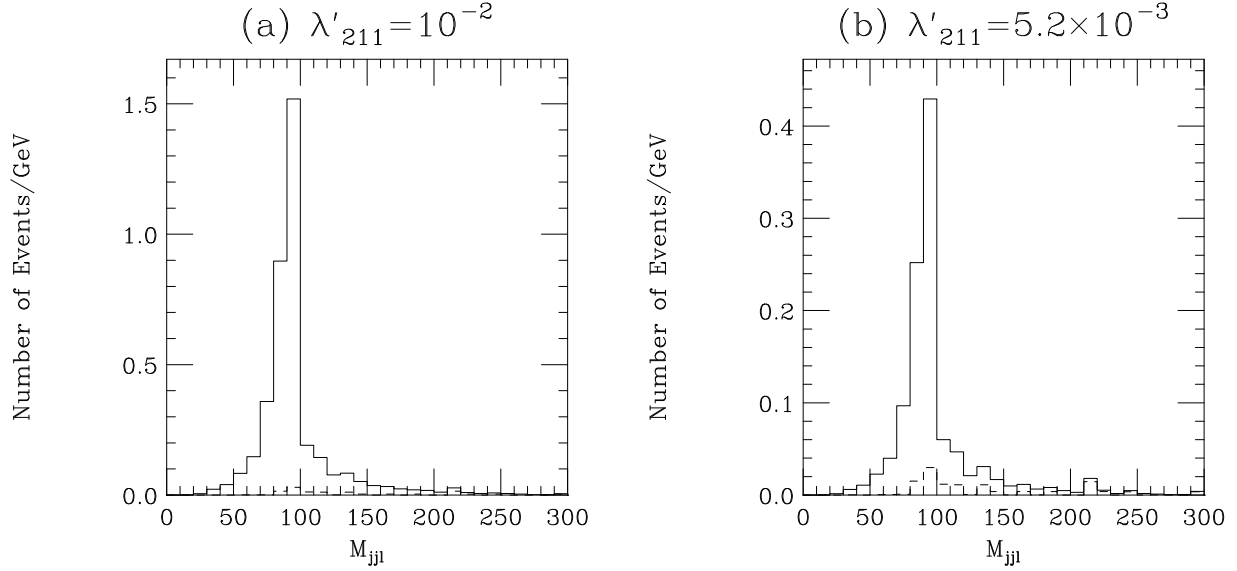


Figure 24: The reconstructed neutralino mass at the Tevatron for  $M_0 = 50$  GeV,  $M_{1/2} = 250$  GeV,  $\tan\beta = 2$ ,  $\text{sgn}\mu > 0$  and  $A_0 = 0$  GeV. The value of the coupling in (b) is chosen such that after the cuts applied in Section 4.1 the signal is  $5\sigma$  above the background. At this point the lightest neutralino mass is  $M_{\tilde{\chi}_1^0} = 98.9$  GeV. We have again normalized the distributions to an integrated luminosity of  $2 \text{ fb}^{-1}$ . The dashed line shows the background and the solid line the sum of the signal and the background.

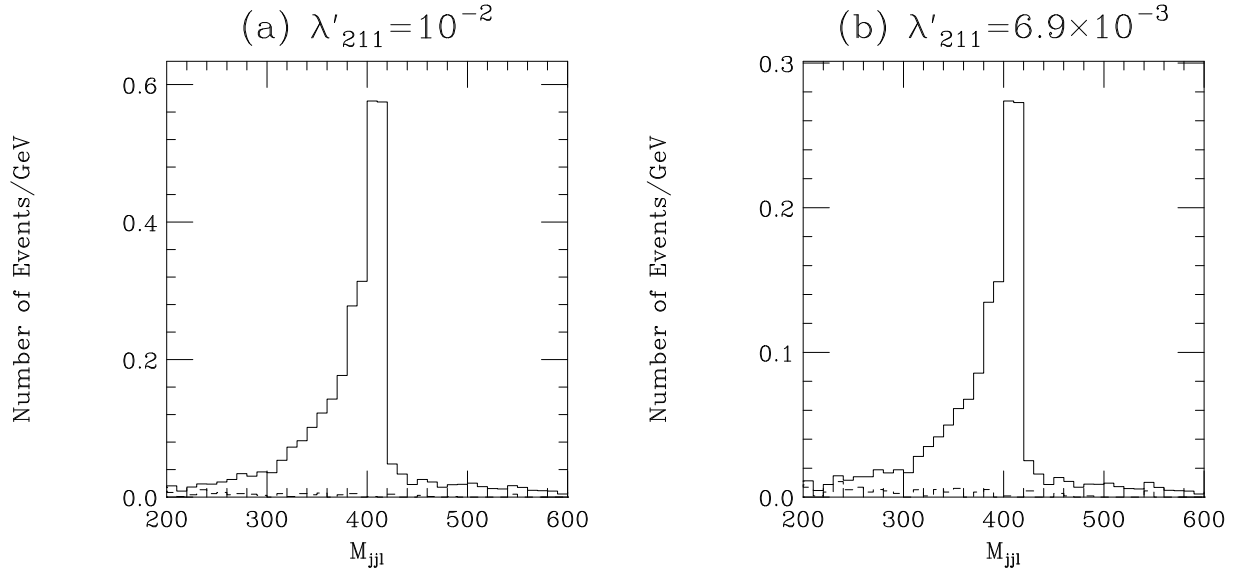


Figure 25: The reconstructed neutralino mass at the LHC for  $M_0 = 350$  GeV,  $M_{1/2} = 950$  GeV,  $\tan\beta = 10$ ,  $\text{sgn}\mu < 0$  and  $A_0 = 0$  GeV. The value of the coupling in (b) is chosen such that after the cuts applied in Section 4.2 the signal is  $5\sigma$  above the background. At this point the lightest neutralino mass is  $M_{\tilde{\chi}_1^0} = 418.0$  GeV. We have again normalized the distributions to an integrated luminosity of  $10 \text{ fb}^{-1}$ . The dashed line shows the background and the solid line the sum of the signal and the background.

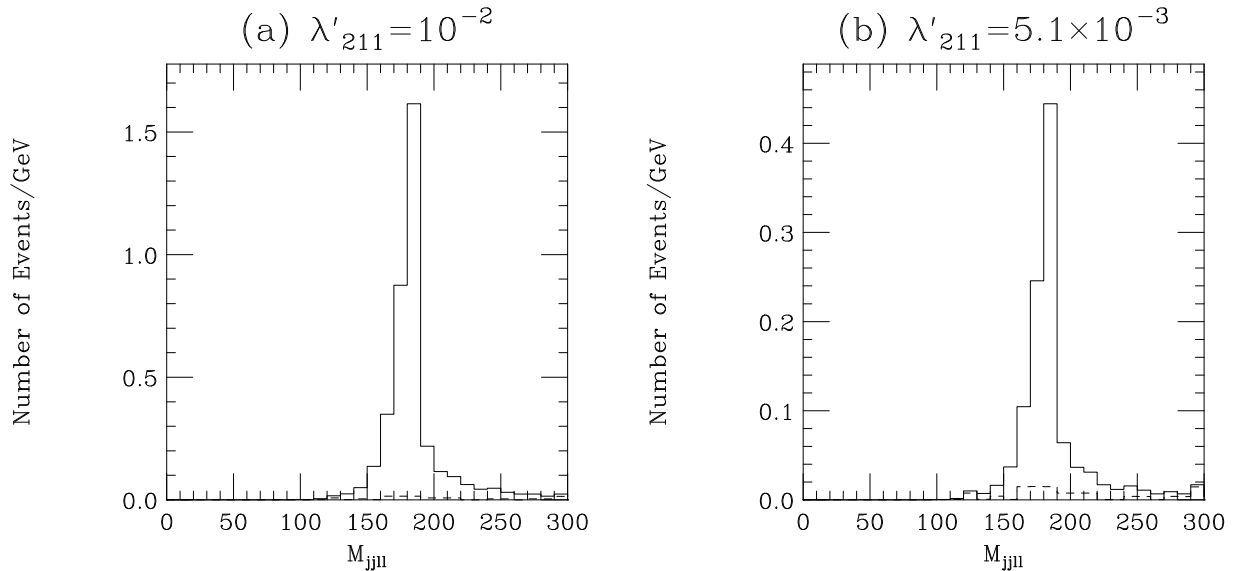


Figure 26: The reconstructed slepton mass at the Tevatron for  $M_0 = 50$  GeV,  $M_{1/2} = 250$  GeV,  $\tan\beta = 2$ ,  $\text{sgn}\mu > 0$  and  $A_0 = 0$  GeV. The value of the coupling in (b) is chosen such that after the cuts applied in Section 4.1 the signal is  $5\sigma$  above the background. At this point the smuon mass is  $M_{\tilde{\mu}_L} = 189.1$  GeV. We have again normalized the distributions to an integrated luminosity of  $2 \text{ fb}^{-1}$ . The dashed line shows the background and the solid line the sum of the signal and the background.

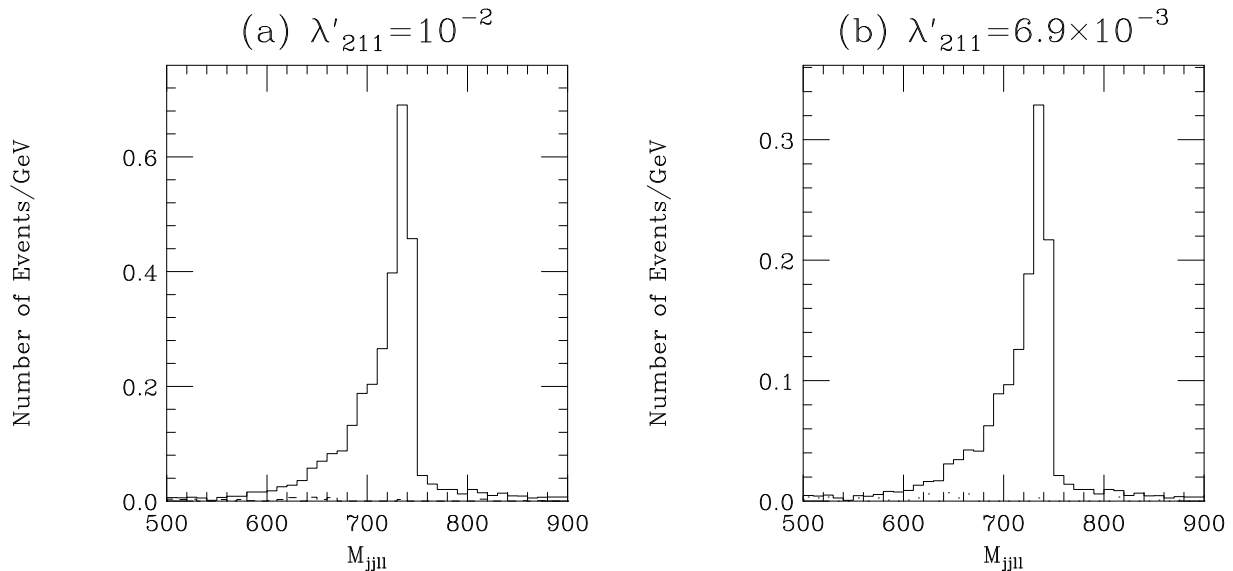


Figure 27: The reconstructed slepton mass at the LHC for  $M_0 = 350$  GeV,  $M_{1/2} = 950$  GeV,  $\tan\beta = 10$ ,  $\text{sgn}\mu < 0$  and  $A_0 = 0$  GeV. The value of the coupling in (b) is chosen such that after the cuts applied in Section 4.2 the signal is  $5\sigma$  above the background. At this point the smuon mass is  $M_{\tilde{\mu}_L} = 745.9$  GeV. We have again normalized the distributions to an integrated luminosity of  $10 \text{ fb}^{-1}$ . The dashed line shows the background and the solid line the sum of the signal and the background.

Experiment	$\lambda'_{211}$	Cuts	Point	Neutralino mass/ GeV		Slepton mass/ GeV	
				Actual	Recon.	Actual	Recon.
Tevatron	$10^{-2}$	no	A	98.9	90.3	189.1	181.6
Tevatron	$5.2 \times 10^{-3}$	no	A	98.9	91.8	189.1	182.3
LHC	$10^{-2}$	no	B	418.0	404.1	745.0	734.1
LHC	$6.9 \times 10^{-2}$	no	B	418.0	405.1	745.0	732.6
LHC	$10^{-2}$	no	C	147.6	142.7	432.0	421.3
LHC	$10^{-2}$	yes	C	147.6	143.4	432.0	423.3

Table 4: Reconstructed neutralino and slepton masses. The following SUGRA points were used in these simulations: point A has  $M_0 = 50$  GeV,  $M_{1/2} = 250$  GeV,  $\tan \beta = 2$ ,  $\text{sgn } \mu > 0$  and  $A_0 = 0$  GeV; point B has  $M_0 = 350$  GeV,  $M_{1/2} = 950$  GeV,  $\tan \beta = 10$ ,  $\text{sgn } \mu < 0$  and  $A_0 = 0$  GeV; point C has  $M_0 = 350$  GeV,  $M_{1/2} = 350$  GeV,  $\tan \beta = 10$ ,  $\text{sgn } \mu < 0$  and  $A_0 = 0$  GeV. The Tevatron and LHC results are based on  $2 \text{ fb}^{-1}$  and  $10 \text{ fb}^{-1}$  integrated luminosity, respectively.

$M_{1/2} = 250$  GeV,  $\tan \beta = 2$ ,  $\text{sgn } \mu > 0$  and  $A_0 = 0$  GeV the branching ratio for the decay of the smuon to the lightest neutralino is  $\text{BR}(\tilde{\mu}_L \rightarrow \tilde{\chi}_1^0 \mu^+) = 98\%$ . Similarly at the point  $M_0 = 350$  GeV,  $M_{1/2} = 950$  GeV,  $\tan \beta = 10$ ,  $\text{sgn } \mu < 0$  and  $A_0 = 0$  GeV the dominant decay mode of the smuon is to the lightest neutralino,  $\text{BR}(\tilde{\mu}_L \rightarrow \tilde{\chi}_1^0 \mu^+) = 99\%$ .

It can however be the case that there is a significant background from sparticle pair production and a substantial contribution from the production of charginos and heavier neutralinos. This is shown in Fig. 28a for the neutralino mass reconstruction and Fig. 29a for the smuon mass reconstruction. As can be seen in the Figs. 28a and 29a there is a significant background in both distributions. At this point, *i.e.*  $\lambda'_{211} = 10^{-2}$ ,  $M_0 = 350$  GeV,  $M_{1/2} = 350$  GeV,  $\tan \beta = 10$ ,  $\text{sgn } \mu < 0$  and  $A_0 = 0$  GeV, the smuon dominantly decays to the lightest chargino,  $\text{BR}(\tilde{\mu}_L \rightarrow \tilde{\chi}_1^- \nu_\mu) = 50.9\%$ , with the other important decay modes being to the next-to-lightest neutralino,  $\text{BR}(\tilde{\mu}_L \rightarrow \tilde{\chi}_2^0 \mu^+) = 28.0\%$ , and the lightest neutralino  $\text{BR}(\tilde{\mu}_L \rightarrow \tilde{\chi}_1^0 \mu^+) = 20.9\%$ . In the neutralino distribution there is still a peak at the simulated neutralino mass, although there is a large tail at higher masses. This tail is mainly due to the larger sparticle pair production background. The production of charginos and the heavier neutralinos does not significantly effect this distribution as the heavier gauginos will cascade decay to the LSP due to the small  $\mathcal{R}_p$  coupling.

In the slepton distribution in addition to the larger background there is also a spurious peak in the mass distribution due to the production of the the lightest chargino and the  $\tilde{\chi}_2^0$ . As we are not including all the decay products of the chargino or  $\tilde{\chi}_2^0$  in the mass reconstruction the reconstructed slepton mass in signal events where a chargino or heavier neutralino is produced is below the true value.

We can improve the extraction of both the neutralino and slepton masses by imposing some additional cuts. The aim of these cuts is to require that the neutralino candidate and the second lepton are produced back-to-back, because in most of the signal events the resonant smuon will only have a small transverse momentum due to the initial-state



parton shower. We therefore require the transverse momenta of the neutralino candidate and the second lepton to satisfy  $|p_T^{\text{jj}\ell_1} - p_T^{\ell_2}| < 20$  GeV, and the azimuthal angles to satisfy  $|\phi_{\text{jj}\ell_1} - \phi_{\ell_2} - 180^\circ| < 15^\circ$ .  $p_T^{\text{jj}\ell_1}$  is the transverse momentum of the combination of the hardest two jets in the event and the lepton closest to the jets in  $(\eta, \phi)$  space, *i.e.* the transverse momentum of the neutralino candidate. Similarly  $\phi_{\text{jj}\ell_1}$  is the azimuthal angle of the combination of the hardest two jets in the event and the lepton closest to the jets in  $(\eta, \phi)$  space, *i.e.* the azimuthal angle of the neutralino candidate.

As can be seen in both Figs. 28b and 29b this significantly reduces the background and the spurious peak in the slepton mass distribution. At these points it is also possible to reconstruct the lightest neutralino, chargino and sneutrino masses using the decay chain  $\tilde{\nu} \rightarrow \tilde{\chi}_1^+ \ell^+$  followed by the decay of the chargino  $\tilde{\chi}_1^+ \rightarrow \ell^+ \nu_\ell \tilde{\chi}_1^0$  and the  $\mathcal{R}_p$  decay of the lightest neutralino to a lepton and two jets [22, 23]. The reconstructed neutralino and slepton masses, before and after the imposition of the new cuts, are given in Table 4. The same procedure as before was used to extract the sparticle masses. There is reasonable agreement between the simulated and reconstructed sparticle masses although again the reconstructed values lie between 5 and 15 GeV below the values used in the simulations, due to the loss of energy from the cones used to define the jets in the neutralino decay.

## 5 Conclusions

We have performed a detailed analysis of the background to like-sign dilepton production at both Run II of the Tevatron and the LHC. We find a background from Standard Model processes of  $0.43 \pm 0.16$  events for  $2 \text{ fb}^{-1}$  integrated luminosity at the Tevatron and  $4.9 \pm 1.6$  events for  $10 \text{ fb}^{-1}$  integrated luminosity at the LHC after a set of cuts. If we only consider this background there are large regions of SUGRA parameter space where resonant slepton production followed by a supersymmetric gauge decay of the slepton is visible above the SM background even for the small values of the  $\mathcal{R}_p$  couplings we considered.

This is presumably the strategy which would be adopted in any initial experimental search, *i.e.* looking for an excess of a given type of event over the Standard Model prediction. If such an excess were observed it would then be necessary to identify which of the many possible models of beyond the Standard Model physics was correct.

In the  $\mathcal{R}_p$  MSSM such an excess of like-sign dileptons can come from two possible sources, from sparticle pair production followed by the decay of the LSP, and from resonant sparticle production. We have considered the background to resonant slepton production from sparticle pair production and found that after an additional cut on the number of jets the signal from resonant slepton production is visible above the combined Standard Model and SUSY pair production background for large ranges of SUGRA parameter space. Finally we have studied the possibility of measuring the mass of the resonant slepton and the neutralino into which it decays. Our results suggest that this should be possible even if the signal is only just detectable above the background.

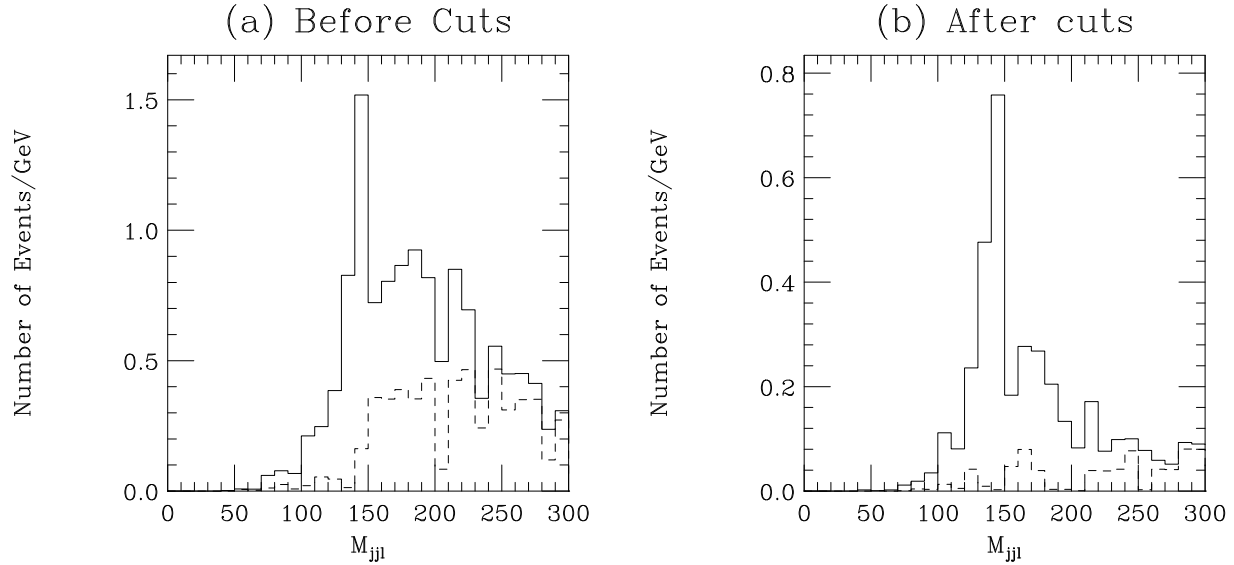


Figure 28: The reconstructed neutralino mass at the LHC for  $\lambda'_{211} = 10^{-2}$ ,  $M_0 = 350$  GeV,  $M_{1/2} = 350$  GeV,  $\tan\beta = 10$ ,  $\text{sgn}\mu < 0$  and  $A_0 = 0$  GeV. At this point the lightest neutralino mass is  $M_{\tilde{\chi}_1^0} = 147.6$  GeV. We have again normalized the distributions to an integrated luminosity of  $10 \text{ fb}^{-1}$ . The cuts used are described in the text. The dashed line shows the background and the solid line the sum of the signal and the background.

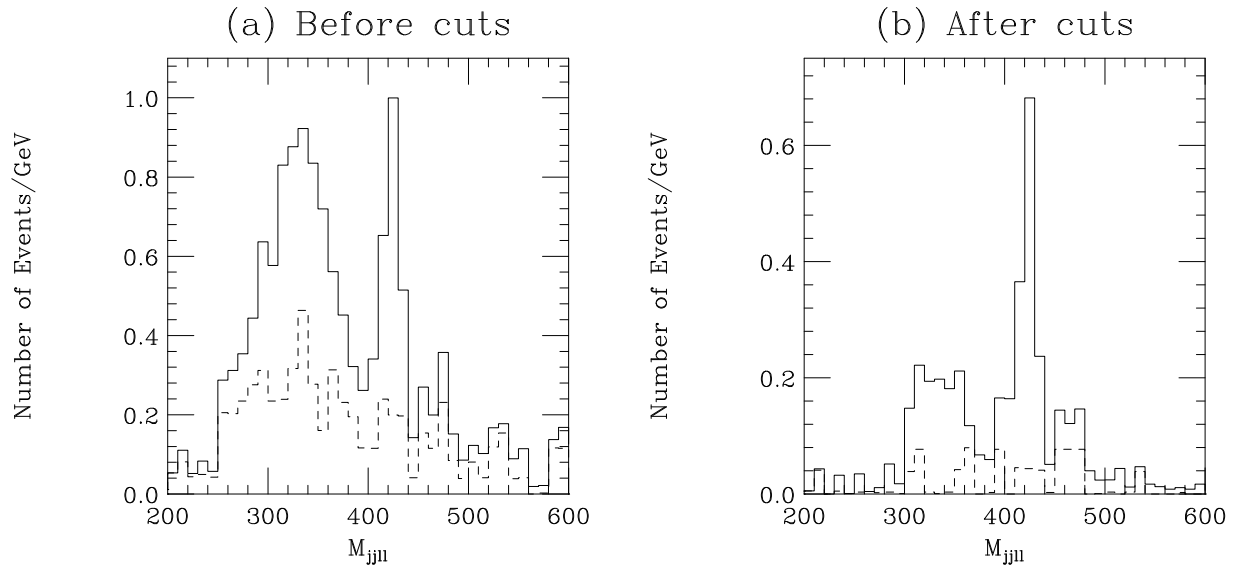


Figure 29: The reconstructed slepton mass at the LHC for  $\lambda'_{211} = 10^{-2}$ ,  $M_0 = 350$  GeV,  $M_{1/2} = 350$  GeV,  $\tan\beta = 10$ ,  $\text{sgn}\mu < 0$  and  $A_0 = 0$  GeV. At this point the smuon mass is  $M_{\tilde{\mu}_L} = 432.0$  GeV. We have again normalized the distributions to an integrated luminosity of  $10 \text{ fb}^{-1}$ . The cuts used are described in the text. The dashed line shows the background and the solid line the sum of the signal and the background.

## Acknowledgments

We would like to thank the organizers of the Tevatron Run II workshop on supersymmetry and Higgs physics for motivating us to start this work. We thank R. Thorne for helpful discussions. P. Richardson would like to thank PPARC for a research studentship, number PPA/S/S/1997/02517.

## References

- [1] H. Dreiner, in *Perspectives on Supersymmetry*, ed. G.L. Kane, World Scientific, (1997), hep-ph/9707435; G. Bhattacharyya, (1997), hep-ph/9709395; R. Barbier *et al.*, (1998), hep-ph/9810232.
- [2] B. C. Allanach, A. Dedes, and H. K. Dreiner, Phys. Rev. **D60**, 075014 (1999), hep-ph/9906209.
- [3] S. Dimopoulos and L. J. Hall, Phys. Lett. **B207**, 210 (1988).
- [4] V. Barger, G. F. Giudice, and T. Han, Phys. Rev. **D40**, 2987 (1989).
- [5] H. Dreiner and S. Lola, (1992), OUTP-92-02-P.
- [6] G. F. Giudice *et al.*, (1996), hep-ph/9602207.
- [7] ECFA/DESY LC Physics Working Group, E. Accomando *et al.*, Phys. Rept. **299**, 1 (1998), hep-ph/9705442.
- [8] J. Erler, J. L. Feng, and N. Polonsky, Phys. Rev. Lett. **78**, 3063 (1997), hep-ph/9612397.
- [9] J. Kalinowski, R. Rückl, H. Spiesberger, and P. M. Zerwas, Phys. Lett. **B406**, 314 (1997), hep-ph/9703436.
- [10] S. Dimopoulos, R. Esmailzadeh, L. J. Hall, and G. D. Starkman, Phys. Rev. **D41**, 2099 (1990).
- [11] H. Dreiner and G. G. Ross, Nucl. Phys. **B365**, 597 (1991).
- [12] H. Dreiner, P. Richardson, and M. H. Seymour, JHEP **0004**, 008 (2000), hep-ph/9912407.
- [13] B. C. Allanach *et al.*, (1999), hep-ph/9906224.
- [14] A. Datta, J. M. Yang, B.-L. Young, and X. Zhang, Phys. Rev. **D56**, 3107 (1997), hep-ph/9704257.
- [15] J.-M. Yang *et al.*, (1997), hep-ph/9802305.

- [16] R. J. Oakes, K. Whisnant, J. M. Yang, B.-L. Young, and X. Zhang, Phys. Rev. **D57**, 534 (1998), hep-ph/9707477.
- [17] E. L. Berger, B. W. Harris, and Z. Sullivan, Phys. Rev. Lett. **83**, 4472 (1999), hep-ph/9903549.
- [18] J. Butterworth and H. Dreiner, Nucl. Phys. **B397**, 3 (1993), hep-ph/9211204; H. Dreiner and P. Morawitz, Nucl. Phys. **B428**, 31 (1994), hep-ph/9405253; H. Dreiner and P. Morawitz, Nucl. Phys. **B503**, 55 (1997), hep-ph/9703279; G. Altarelli, J. Ellis, G. F. Giudice, S. Lola, and M. L. Mangano Nucl. Phys. **B506**, 3 (1997), hep-ph/9703276; J. Kalinowski, R. Rückl, H. Spiesberger, and P. M. Zerwas Z. Phys. **C74**, 595 (1997), hep-ph/9703288.
- [19] J. Kalinowski, R. Rückl, H. Spiesberger, and P. M. Zerwas Phys. Lett. **B414**, 297 (1997), hep-ph/9708272.
- [20] J. L. Hewett and T. G. Rizzo, (1998), hep-ph/9809525.
- [21] H. Dreiner, P. Richardson, and M. H. Seymour, (1998), hep-ph/9903419; H. Dreiner, P. Richardson, and M. H. Seymour, (2000), hep-ph/0001224.
- [22] G. Moreau, M. Chemtob, F. Deliot, C. Royon, and E. Perez, (1999), hep-ph/9910341; G. Moreau, E. Perez, and G. Polesello, (2000), hep-ph/0002130; G. Moreau, E. Perez, and G. Polesello, (2000), hep-ph/0003012.
- [23] S. Abdullin *et al.*, (1999), hep-ph/0005142.
- [24] HERWIG6.1, G. Corcella *et al.*, (1999), hep-ph/9912396; G. Marchesini *et al.*, Comput. Phys. Commun. **67**, 465 (1992).
- [25] S. Moretti *et al.*, Cavendish-HEP-98/06.
- [26] M. Hirsch, H. V. Klapdor-Kleingrothaus, and S. G. Kovalenko, Phys. Rev. Lett. **75**, 17 (1995); M. Hirsch, H. V. Klapdor-Kleingrothaus, and S. G. Kovalenko, Phys. Rev. **D53**, 1329 (1996), hep-ph/9502385; K. S. Babu and R. N. Mohapatra, Phys. Rev. Lett. **75**, 2276 (1995), hep-ph/9506354.
- [27] J. Ellis, J. S. Hagelin, D. V. Nanopoulos, K. Olive, and M. Srednicki, Nucl. Phys. **B238**, 453 (1984).
- [28] OPAL, G. Abbiendi *et al.*, Eur. Phys. J. **C11**, 619 (1999), hep-ex/9901037.
- [29] OPAL, G. Abbiendi *et al.*, Eur. Phys. J. **C12**, 1 (2000), hep-ex/9904015.
- [30] ALEPH, R. Barate *et al.*, Eur. Phys. J. **C7**, 383 (1999), hep-ex/9811033.
- [31] H. Baer, F. E. Paige, S. D. Protopopescu, and X. Tata, (1999), hep-ph/0001086.

- [32] S. Dawson, Nucl. Phys. **B261**, 297 (1985).
- [33] H. Baer, M. Bisset, X. Tata, and J. Woodside, Phys. Rev. **D46**, 303 (1992); H. Baer, X. Tata, and J. Woodside, Phys. Rev. **D45**, 142 (1992).
- [34] C. Albajar *et al.*, In \*Aachen 1990, Proceedings, Large Hadron Collider, vol. 2\* 621-653. CERN Geneva - CERN-90-10-B, 621- 653.
- [35] V. Barger, W. Y. Keung, and R. J. N. Phillips, Phys. Rev. Lett. **55**, 166 (1985).
- [36] R. M. Barnett, J. F. Gunion, and H. E. Haber, Phys. Lett. **B315**, 349 (1993), hep-ph/9306204.
- [37] H. Dreiner, M. Guchait, and D. P. Roy, Phys. Rev. **D49**, 3270 (1994), hep-ph/9310291; M. Guchait and D. P. Roy, Phys. Rev. **D52**, 133 (1995), hep-ph/9412329.
- [38] ATLAS, W. W. Armstrong *et al.*, CERN-LHCC-94-43.
- [39] H. Baer, M. Drees, C. Kao, M. Nojiri, and X. Tata, Phys. Rev. **D50**, 2148 (1994), hep-ph/9403307.
- [40] H. Baer, C. hao Chen, F. Paige, and X. Tata, Phys. Rev. **D53**, 6241 (1996), hep-ph/9512383.
- [41] S. Abdullin and F. Charles, Nucl. Phys. **B547**, 60 (1999), hep-ph/9811402.
- [42] K. T. Matchev and D. M. Pierce, Phys. Rev. **D60**, 075004 (1999), hep-ph/9904282.
- [43] K. T. Matchev and D. M. Pierce, Phys. Lett. **B467**, 225 (1999), hep-ph/9907505.
- [44] CDF, J. Nachtman, D. Saltzberg, and M. Worcester, (1999), hep-ex/9902010.
- [45] H. Baer, M. Drees, F. Paige, P. Quintana, and X. Tata, Phys. Rev. **D61**, 095007 (2000), hep-ph/9906233.
- [46] N. K. Mondal and D. P. Roy, Phys. Rev. **D49**, 183 (1994), hep-ph/9305344; R. M. Godbole, S. Pakvasa, and D. P. Roy, Phys. Rev. Lett. **50**, 1539 (1983); V. Barger, A. D. Martin, and R. J. N. Phillips, Phys. Rev. **D28**, 145 (1983); D. P. Roy, Phys. Lett. **196B**, 395 (1987).
- [47] PYTHIA6.1, T. Sjostrand, Comput. Phys. Commun. **82**, 74 (1994).
- [48] J. M. Campbell and R. K. Ellis, Phys. Rev. **D60**, 113006 (1999), hep-ph/9905386.
- [49] R. Bonciani, S. Catani, M. L. Mangano, and P. Nason, Nucl. Phys. **B529**, 424 (1998), hep-ph/9801375.
- [50] S. Frixione and G. Ridolfi, Nucl. Phys. **B507**, 315 (1997), hep-ph/9707345.

- [51] M. L. Mangano, P. Nason, and G. Ridolfi, Nucl. Phys. **B373**, 295 (1992).
- [52] A. D. Martin, R. G. Roberts, W. J. Stirling, and R. S. Thorne, Eur. Phys. J. **C14**, 133 (2000), hep-ph/9907231; A. D. Martin, R. G. Roberts, W. J. Stirling, and R. S. Thorne, Eur. Phys. J. **C4**, 463 (1998), hep-ph/9803445.